tant Ad vector containing the AB loop mutation was found to mediate significantly lower tissue transduction *in vivo*. Furthermore, this mutant Ad vector reduced (or blunted) liver toxicity and innate immunity responses (interleukin-6 production). Thus, the triple-mutant Ad vector will likely be a fundamental vector for targeted gene delivery.

INTRODUCTION

RECOMBINANT ADENOVIRAL (Ad) VECTORS are attractive vehicles for *in vitro* and *in vivo* gene transfer to a wide variety of cell types. This distribution is largely due to the relatively broad expression of the primary receptor, the coxsackievirus and adenovirus receptor (CAR), and the secondary receptor, α_v integrin, and the tertiary receptor, heparan sulfate glycosaminoglycans (HSGs). The lack of specificity limits the utility of Ad vectors in gene therapy. Targeted Ad vectors would improve not only the efficacy but also the safety profiles of the vectors by permitting the use of lower doses, which would be less toxic and potentially less immunogenic (Krasnykh *et al.*, 2000; Wickham, 2000; Mizuguchi and Hayakawa, 2004).

The initial phase of Ad infection involves at least two sequential steps. The first is attachment of the virus to the cell surface through binding of the knob domain of the fiber to CAR (Bergelson *et al.*, 1997; Tomko *et al.*, 1997). After attachment, interaction between the RGD motif of the penton bases with secondary host cell receptors, α_v integrins, facilitates internalization via receptor-mediated endocytosis (Wickham *et al.*, 1993, 1994). Furthermore, interaction between the KKTK (Lys-Lys-Thr-Lys) motif on the fiber shaft of Ad type 5 with HSGs and the length of the fiber shaft are involved in accumulation, in mouse and cynomolgus monkey liver, of systemically administered Ad vectors (Nakamura *et al.*, 2003; Smith *et al.*, 2003a,b; Vigne *et al.*, 2003).

Strategies to eliminate natural Ad tropism, based on modification of particular viral capsid proteins such as fiber and penton base (Wickham, 2000; Mizuguchi and Hayakawa, 2004), have been reported. To ablate CAR binding, Ad vectors containing an AB, DE, or FG loop mutation of the fiber knob (Bewley *et al.*, 1999; Kirby *et al.*, 1999; Alemany and Curiel, 2001; Einfeld *et al.*, 2001; Leissner *et al.*, 2001; Mizuguchi *et al.*, 2002; Smith *et al.*, 2002), Ad vectors containing the Ad type 40 short fiber (which has been hypothesized not to bind to any receptors; Nakamura *et al.*, 2003), and Ad vectors containing an external trimerization motif instead of the fiber knob (Hong *et al.*, 2003) have been developed. To ablate α_v integrin binding, Ad vectors with a deletion of the RGD (Arg-Gly-Asp) motif of the penton base (Einfeld *et al.*, 2001; Mizuguchi *et al.*, 2002; Vigne *et al.*, 2003) have been developed. To ablate HSG binding, Ad vectors mutated in the KKTK motif of the fiber shaft (Smith *et al.*, 2003b) have been developed.

Several groups have reported that Ad vectors from which CAR binding has been ablated do not change the biodistribution of Ad vectors (Alemany and Curiel, 2001; Leissner *et al.*, 2001; Mizuguchi *et al.*, 2002; Smith *et al.*, 2002), although Einfeld *et al.* have reported that CAR binding-ablated Ad vectors exhibit a 10-fold decrease in liver transduction (Einfeld *et al.*, 2001). Einfeld *et al.* have also reported that Ad vectors ablated for both CAR binding ablation and α_v integrin binding exhibit a more than 700-fold decrease in liver transduction (Einfeld *et al.*, 2001). Ad vectors ablated for α_v integrin binding, however, do not change their biodistribution (Mizuguchi *et al.*, 2002; Smith *et al.*, 2003b). Smith *et al.* have shown that HSG binding-ablated Ad vectors, in which the KKTK motif on the fiber shaft of Ad type 5 is changed to GAGA (Gly-Ala-Gly-Ala), exhibit a 15-fold decrease in liver transduction (Smith *et al.*, 2003b).

We have previously developed an Ad vector ablated for CAR, α_v integrin, and HSG binding by deleting four amino acids (T489, A490, Y491, and T492) from the FG loop of the fiber knob, deleting the RGD motif of the penton base, and substituting the fiber shaft domain for that derived from Ad type 35, which does not contain the HSG-binding motif (Koizumi *et al.*, 2003a). This triple-mutant Ad vector, on intravenous administration, showed more than 1000-fold lower gene transfer activity in mouse liver than the conventional Ad vector whereas double-mutant Ad vectors (ablated for CAR and α_v integrin binding, or for CAR and HSG binding), on intravenous administration, showed 100-fold lower gene transfer activity in mouse liver than the conventional Ad vector (Koizumi *et al.*, 2003a).

In the present study, we further improve the triple-mutant Ad vector by adding a mutation of the AB loop in the fiber knob (R412S, A415G, E416G, and K417G) instead of a deletion of the FG loop in the fiber knob. The AB loop in the fiber knob interacts directly with CAR and therefore must be the key anchor for the knob–CAR complex (Bewley *et al.*, 1999). In contrast, deletion of the FG loop in the fiber knob eliminates interactions between the fiber knob and CAR by changing the structure of the fiber knob (Kirby *et al.*, 1999). We examined in detail the gene transfer activity of the triple-mutant Ad vector containing a mutation of the AB loop in the fiber knob both *in vitro* and *in vivo* (intravenous and intraperitoneal administration) in comparison with the triple-mutant Ad vector containing a deletion of the FG loop in the fiber knob and the conventional Ad vector.

Another drawback of the Ad vector is the production (release) of cytokines and chemokines, as well as hepatotoxicity, after systemic injection of the vector (Lieber *et al.*, 1997; Liu *et al.*, 2003). The cytokines play a major causative role in liver damage associated with systemic Ad infusion as well as a role in the induction of an antiviral immune response. Cytokine production and release are thought to be the direct or indirect results of Ad uptake by Kupffer cells and their subsequent activation (Lieber *et al.*, 1997; Liu *et al.*, 2003) or lysis (Schiedner *et al.*, 2003). It is important to develop an Ad vector that reduces or blunts innate immune response. In the present study, we also show that systemic injection of the triple-mutant Ad vector does not increase serum interleukin (IL)-6 levels or liver serum enzymes (aspartate aminotransferase [AST] and alanine aminotransferase [ALT], which are hepatotoxicity marker enzymes).

MATERIALS AND METHODS

Cells

SK HEP-1 (endothelial cell line derived from human liver; Heffelfinger *et al.*, 1992) and 293 cells were cultured with Dulbecco's modified Eagle's medium (DMEM) supplemented with 10% fetal calf serum (FCS). Fiber-293 cells, which are stable transformants expressing Ad type 5 fiber protein (Koizumi *et al.*,

2003a), were cultured with DMEM supplemented with 10% FCS and hygromycin (GIBCO, 200 μg/ml; Invitrogen, Carlsbad, CA).

Plasmids and Ad vectors

The vector plasmid pAdHM59, which we used to generate Ad vectors containing a mutation of the AB loop of the fiber knob (R412S, A415G, E416G, and K417G), a deletion of the RGD motif in the penton base, and a substitution of the fiber shaft domain for that derived from Ad type 35, was constructed as follows. First, a polymerase chain reaction (PCR) fragment containing a sequence surrounding the AB loop of the Ad type 5 fiber knob gene (bp 32238–32495) was generated with primers (forward, 5′-ATTAATACTTTGTGGACCACACC-AGCTCCATCTCCTAACTGTAGcCTAAATGgAGgGggt-GATGCTAAACTCACTTTGGTCTTAACAAAA-3′ [the *Ase*I site is underlined and the mutation sequence is indicated by lower-case letters]; reverse, 5′-AGATCTCCATTTCTAAAG-TT-3′ [the *Bgl*II site is underlined]) and pGEM-Teasy-knob-CAR(+) as a template (Koizumi *et al.*, 2003a). The PCR fragment was then ligated with *Eco*RV-digested pcDNA3.1-Hygro (Invitrogen), resulting in pcDNA3.1-Hyg-AB4m. pcDNA3.1-Hyg-AB4mknob was constructed by three-piece ligation of (1) the *Afl*II/*Ase*I fragment of pF35-2.3(AseI) (Mizuguchi and Hayakawa, 2002), which contains the fiber shaft of Ad type 35, (2) the *Ase*I/*Bgl*II fragment of pcDNA3.1-Hyg-AB4m, and (3) the *Afl*II/*Bgl*II fragment of pcDNA3.1-Hygro. Next, pHM-S35-K5-AB4m was constructed by three-piece ligation of (1) the *Afl*II/*Bgl*II fragment of pcDNA3.1-Hyg-AB4mknob, (2) the *Mun*I/*Bgl*II fragment of pHM-S35-K5-CAR(+) (Koizumi *et al.*, 2003a), and (3) the *Afl*II/*Mun*I fragment of pHMCMV6 (Mizuguchi and Kay, 1999). pHM-S35-K5-AB4m contains the sequence encoding the CAR-binding ablated Ad type 5 fiber knob (mutation of the sequence encoding four amino acids in the AB loop), a *Csp*45I site in the HI loop, a *Cla*I site in the C-terminal end of the fiber knob-coding sequence, and the fiber shaft sequence of Ad type 35. pS35-K5-2.2-AB4m was then constructed by ligation of *Srf*I/*Mun*I-digested pHM14-Eco2 (Koizumi *et al.*, 2003b) and *Srf*I/*Mun*I-digested pHM-S35-K5-AB4m. Next, the *Srf*I/*Mun*I fragment of pS35-K5-2.2-AB4m was ligated with the *Srf*I/*Mun*I fragment of pHM14-Eco12, resulting in the creation of pHM14-Eco2-S35-AB4m, which contains the Ad genome from bp 27331 to the end of the Ad genome and contains the sequence encoding the substitution of the fiber shaft domain for that derived from Ad type 35 and the mutation of the AB loop of the fiber knob. Finally, pAdHM59 was constructed by ligation of *Eco*RI/*Cla*I-digested pHM14-Eco2-S35-AB4m (the location of the *Eco*RI site is bp 27332 in the Ad genome, whereas the *Cla*I site is in the C-terminal end of the fiber-coding sequence) and *Eco*RI/*Cla*I-digested pAdHM43 (Koizumi *et al.*, 2003a), which contains the complete Ad genome, deletion of the RGD motif in the penton base, and a *Cla*I site in the C-terminal end of the fiber-coding sequence. pAdHM59 has a complete E1/E3-deleted Ad genome with I-*Ceu*I, *Swa*I, and PI-*Sce*I sites in the E1 deletion region, *Pac*I sites at both ends of the Ad genome, and deletion of the RGD peptide-coding sequence of the penton base (MND-HAIRGDTFATRAE was changed to MNDTSRAE), and contains the chimeric fiber-coding sequence of the CAR binding-ablated Ad type 5 fiber knob (mutation of the AB loop-coding region of the fiber knob [R412S, A415G, E416G, and K417G]), the Ad type 35 fiber shaft sequences, and the Ad type 5 fiber tail sequence. pAdHM59 also contains a unique *Csp*45I site in the HI loop of the fiber knob-coding sequence and a *Cla*I site in the C-terminal end of the fiber knob-coding sequence. Therefore, the targeting ligands can be easily displayed in the fiber knob of the vectors by cloning the respective genes into these regions by simple *in vitro* ligation.

Ad vectors were constructed by an improved *in vitro* ligation method described previously (Mizuguchi and Kay, 1998, 1999). pAdHM59-CMVL2 and pAdHM54-CMVL2 were constructed by ligation of I-*Ceu*I/PI-*Sce*I-digested pAdHM59 and pAdHM54, respectively, and I-*Ceu*I/PI-*Sce*I-digested pCMVL1 (Mizuguchi and Kay, 1999). To construct pAdHM59-RGD-CMVL2, pAdHM59 was first digested with *Csp*45I and ligated with oligonucleotide 1 (5′-cggcctgtgactgccgcggagactgtttctgc-gatg-3′) and oligonucleotide 2 (5′-cgcatcgcagaaacagtctccgcg-gcagtcacaggc-3′), which corresponds to the RGD (RGD-4C) peptide, CDCRGDCFC, with high affinities for integrins ($\alpha_v\beta_3$ and $\alpha_v\beta_5$) (Koivunen *et al.*, 1995; Pasqualini *et al.*, 1997), resulting in the creation of pAdHM59-RGD. I-*Ceu*I/PI-*Sce*I-digested pAdHM59-RGD was then ligated with I-*Ceu*I/PI-*Sce*I-digested pCMVL1, resulting in the creation of pAdHM59-RGD-CMVL2.

To generate the virus, pAdHM59-CMVL2, pAdHM54-CMVL2, and pAdHM59-RGD-CMVL2 were digested with *Pac*I and purified by phenol–chloroform extraction and ethanol precipitation. Linearized DNAs were transfected into Fiber-293 cells (in the case of pAdHM54-CMVL2 and pAdHM59-CMVL2) or 293 cells (in the case of pAdHM59-RGD-CMVL2) with Super-Fect (Qiagen, Valencia, CA) according to the manufacturer's instructions. When pAdHM59-CMVL2 and pAdHM54-CMVL2 were transfected into normal 293 cells, the virus was not generated because the virus does not interact with 293 cellular receptors. Viruses [Ad/ΔF(AB)ΔP-S35-L2, Ad/ΔF(FG)ΔP-S35-L2, and Ad/ΔF(AB)ΔP-S35-RGD-L2] were prepared by standard methods with the exception that Ad/ΔF(AB)ΔP-S35-L2 and Ad/ΔF(FG)ΔP-S35-L2 were amplified with Fiber-293 cells, and that only the last step of viral amplification was performed by infection into normal 293 cells, as described previously (Koizumi *et al.*, 2003a). Ad/ΔF(FG)ΔP-S35-L2 is identical to Ad/ΔFΔP-S35-L2 in our previous report (Koizumi *et al.*, 2003a). A conventional luciferase-expressing Ad vector, Ad-L2, had been constructed previously (Mizuguchi and Kay, 1999). Viruses were purified by $CsCl_2$ step gradient ultracentrifugation followed by $CsCl_2$ linear gradient ultracentrifugation. Determination of virus particle titers was accomplished spectrophotometrically by the methods of Maizel *et al.* (1968). Virus particle titers of the vector stocks, prepared from five 150-mm dishes (approximately 8×10^7 cells), were as follows: Ad-L2, 1.8×10^{12} vector particles (VP)/ml; Ad/ΔF(AB)ΔP-S35-L2, 2.8×10^{12} VP/ml; Ad/ΔF(FG)ΔP-S35-L2, 3.3×10^{12} VP/ml; Ad/ΔF(AB)ΔP-S35-RGD-L2, 2.6×10^{12} VP/ml.

Western blotting

Five hundred nanograms of virus in 1× sample buffer containing 4% 2-mercaptoethanol was loaded onto a sodium dodecyl sulfate (SDS)–polyacrylamide gel after boiling for 5 min, followed by electrotransfer to a nitrocellulose membrane. After blocking in Block Ace (Dainippon Pharmaceutical, Osaka, Japan), the filters were incubated with a rabbit fiber knob polyclonal antibody (diluted 1:3000) (kindly provided by R.D. Gerard, University of

Texas Southwestern Medical Center, Dallas, TX), followed by incubation in the presence of peroxidase-labeled anti-rabbit antibody (diluted 1:10,000) (Cell Signaling Technology, Beverly, MA). The filters were developed by chemiluminescence (ECL Western blotting detection system; GE Healthcare, Little Chalfont, UK), and signals were read with an LAS-3000 imaging system (Fujifilm Medical Systems USA, Stamford, CT).

Adenovirus-mediated gene transduction into cultured cells

SK HEP-1 cells (1×10^4 cells) were seeded in a 96-well dish. On the next day, they were transduced with Ad-L2, Ad/ΔF(FG)ΔP-S35-L2, Ad/ΔF(AB)ΔP-S35-L2, or Ad/ΔF(AB)ΔP-S35-RGD-L2 (3000 VP/cell) for 1.5 hr. After a 48-hr culture period, luciferase production in the cells was measured with a luciferase assay system (PicaGene LT2.0 luminescence kit; Toyo Ink, Tokyo, Japan).

In the experiment to quantify Ad uptake into SK HEP-1 cells, the cells were incubated at 37°C for 1.5 hr with the corresponding virus, washed with phosphate-buffered saline (PBS), resuspended in 0.05% trypsin–0.5 m*M* EDTA-PBS solution, and incubated at 37°C for 10 min. After this incubation, the cells were incubated at 37°C for 10 min with 0.05% DNase I–0.5 *M* $MgCl_2$–PBS, washed with PBS, and resuspended in 0.1 *M* EDTA–PBS solution. Finally, the Ad genome DNA in the cells was quantified with a TaqMan fluorogenic detection system (ABI PRISM 7700 sequence detector; Applied Biosystems, Foster City, CA). Sample DNA was isolated with an automatic nucleic acid isolation system (NA-2000; Kurabo Industries, Osaka, Japan). The Ad vector DNA standard was pAdHM4 plasmid DNA (Mizuguchi and Kay, 1999). Primers for amplification were located in the E4 region, with the sequences CACCACCTCCCGGTACCATA (sense) and CCGCACCTGGTTTTGCTT (antisense). The fluorogenic detection probe had the sequence AACCTGCCCGCCGGCTATACACTG. Samples were amplified in 50 μl for 40 cycles in the ABI PRISM 7700 sequence detector with continuous fluorescence monitoring. Data were processed with ABI PRISM 7000 SD software (Applied Biosystems).

When SK HEP-1 cells were transfected with a complex of Ad/ΔF(AB)ΔP-S35-L2 and SuperFect (Qiagen), the cells (2×10^4 cells) were seeded in a 48-well dish. The next day, the cells were transduced with Ad/ΔF(AB)ΔP-S35-L2 (10,000 VP/cell) in the presence of SuperFect (0, 0.15, or 1.5 μg; Qiagen) for 1.5 hr. After a 48-hr culture period, luciferase production in the cells was measured with a luciferase assay system (PicaGene PGL5500; Toyo Ink).

In the competition experiments, SK HEP-1 cells (2×10^4 cells) were seeded in a 48-well dish. The next day, the cells were preincubated with RGD peptide (GRGDSP; TaKaRa, Osaka, Japan) (0, 40, or 200 μg/ml) for 10 min at room temperature. The cells were then transduced with Ad/ΔF(AB)ΔP-S35-RGD-L2 (300 VP/cell) for 0.5 hr. After 48 hr in culture, luciferase production in the cells was measured by luminescence assay (PicaGene LT2.0; Toyo Ink).

Adenovirus-mediated gene transduction in vivo

Ad-L2, Ad/ΔF(FG)ΔP-S35-L2, Ad/ΔF(AB)ΔP-S35-L2, or Ad/ΔF(AB)ΔP-S35-RGD-L2 was intravenously (3.0×10^{10} VP) or intraperitoneally (1.0×10^{11} VP) administered to C57BL/6 mice (male, 5 weeks old; obtained from Nippon SLC, Shizuoka, Japan). Forty-eight hours later, the heart, lung, liver, kidney, and spleen were isolated and homogenized as previously described (Xu *et al.*, 2001). Luciferase production was determined with a luciferase assay system (PicaGene 5500; Toyo Ink). Protein content was measured with a Bio-Rad assay kit (Bio-Rad, Hercules, CA), using bovine serum albumin as a standard.

The amounts of Ad genomic DNA in each organ were quantified with the TaqMan fluorogenic detection system (ABI PRISM 7700 sequence detector; Applied Biosystems). Samples were prepared with isolated DNA templates from each organ (25 ng) by the automatic nucleic acid isolation system (NA-2000; Kurabo Industries). The amounts of Ad DNA were quantified with the TaqMan fluorogenic detection system (Applied Biosystems), as described above.

Amounts of Ad vector DNA in liver parenchymal and nonparenchymal cells

Ad-L2, Ad/ΔF(FG)ΔP-S35-L2, or Ad/ΔF(AB)ΔP-S35-L2 was intravenously (3.0×10^{10} VP) or intraperitoneally (1.0×10^{11} VP) administered to C57BL/6 mice (male, 5 weeks old; Nippon SLC). Mice were anesthetized by intraperitoneal administration of pentobarbital sodium (Dainippon Pharmaceutical) 3 hr after Ad vector injection. Liver cells were separated into parenchymal cells (PCs; hepatocytes) and nonparenchymal cells (NPCs) (Kupffer cells and endothelial cells), as described previously (Nishikawa *et al.*, 1998). Briefly, the liver was perfused with HEPES buffer (pH 7.5) containing collagenase. The dispersed cells were separated into PC and NPC fractions by differential centrifugation. Quantitative PCR was performed to examine the amounts of Ad vector DNA in the PCs and NPCs. Total DNA, including the Ad vector DNA, was isolated from the PCs and NPCs by means of the automatic nucleic acid isolation system (NA-2000; Kurabo Industries). The amounts of Ad DNA were quantified with the TaqMan fluorogenic detection system (Applied Biosystems), as described above.

Blood clearance of Ad vectors

Blood samples were collected by retroorbital bleeding at the indicated times (2, 10, and 30 min; or 2, 60, 120, and 180 min) after intravenous (3.0×10^{10} VP) or intraperitoneal (1.0×10^{11} VP) administration of Ad-L2, Ad/ΔF(FG)ΔP-S35-L2, or Ad/ΔF(AB)ΔP-S35-L2. Total DNA, including the Ad vector DNA, was isolated from whole blood with a QIAamp DNA blood mini kit (Qiagen). The amounts of Ad DNA were quantified with the TaqMan fluorogenic detection system (Applied Biosystems), as described above.

Liver serum enzymes and interleukin-6 levels after systemic administration

Blood samples were collected from the inferior vena cava at the indicated times (3 or 48 hr) after intravenous (3.0×10^{11} VP) or intraperitoneal (1.0×10^{11} VP) administration of Ad-L2, Ad/ΔF(AB)ΔP-S35-L2 or Ad/ΔF(FG)ΔP-S35-L2. Serum samples were collected into separate tubes containing no anticoagulant for coagulation. The levels of AST and ALT in serum samples collected at 48 hr were measured with a Transaminase-CII kit (Wako Pure Chemical Industries, Osaka, Japan). IL-6 levels in serum samples collected 3 hr after Ad injection were

measured with an enzyme-linked immunosorbent assay (ELISA) kit (BioSource International, Camarillo, CA).

RESULTS

Construction of vectors that abolish natural viral tropism is the first step in the development of targeted Ad vectors. Identification and incorporation of a foreign ligand with high affinity for a specific cellular receptor into the capsid of Ad vectors that no longer infect cells would be the next step (Fig. 1A). This study was undertaken to improve a previously developed triple-mutant Ad vector that no longer infects cells by deletion of the FG loop of the fiber knob, deletion of the RGD motif of the penton base, and substitution of the fiber shaft domain with that derived from Ad type 35. Hepatocyte toxicity and innate immune response (IL-6 production) by systemic injection of the vectors were also examined.

Generation of several types of mutant Ad vector

To examine the effects of the various fiber knob mutations (mutation of AB loop or deletion of FG loop) in the triple-mutant Ad vector on gene transfer activity *in vitro* and *in vivo*, we constructed several types of mutant Ad vector expressing luciferase. Ad/ΔF(AB)ΔP-S35-L2 contains the Ad type 5 fiber knob

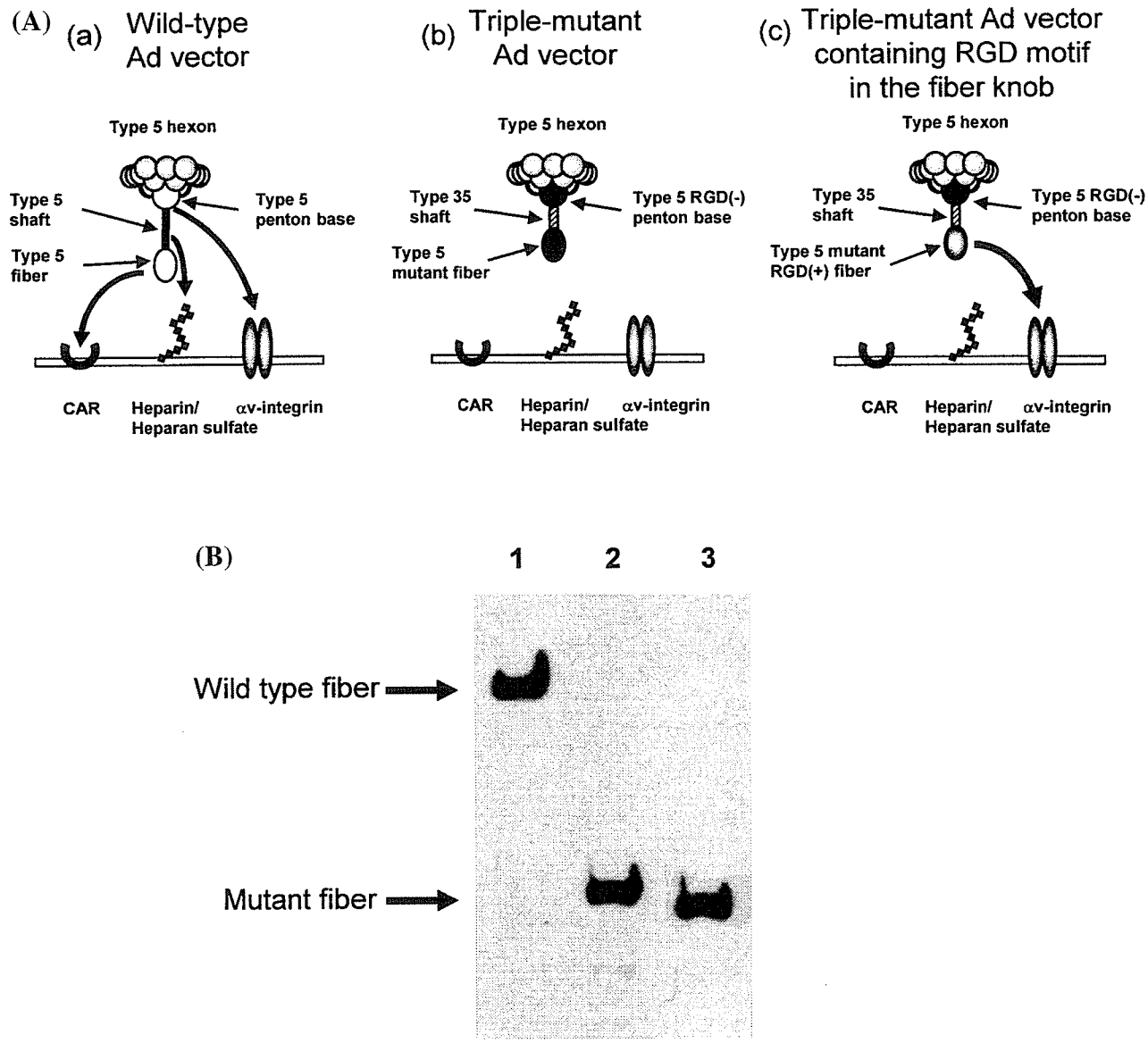

FIG. 1. Mutant Ad vectors. (**A**) Schematic diagram of the interaction of mutant Ad vectors with cells. The wild-type Ad vector infects cells by interactions of the fiber knob with CAR, the fiber shaft with HSGs, and the penton base with α_v integrin. The triple-mutant Ad vector does not have these interactions with cells. The triple-mutant Ad vector containing the RGD motif in the HI loop of the fiber knob infects cells via interaction of the RGD motif with α_v integrin. (**B**) Western blot analysis of the fiber protein in Ad-L2, Ad/ΔF(FG)ΔP-S35-L2, and Ad/ΔF(AB)ΔP-S35-L2. Five hundred nanograms of virus was separated on a 12% SDS–polyacrylamide gel, and the fiber protein was analyzed by Western blotting using a rabbit fiber knob polyclonal antibody as described in Materials and Methods. Lane 1, Ad-L2; lane 2, Ad/ΔF(FG)ΔP-S35-L2; lane 3, Ad/ΔF(AB)ΔP-S35-L2.

TABLE 1. ADENOVIRAL VECTOR MUTATIONS AND POTENTIAL CELL INTERACTIONS

Ad vector	*Amino acid sequence of knob domain*				*Type of Ad shaft*	*Type of Ad tail*	*Penton base*	*Type of Ad vector*[a]
	AB loop	*FG loop*	*HI loop*	*C terminus*				
Conventional Ad								
Ad-L2	–NCRLNAEKDA–	–TEGTAYTNAV–	–DTTPSA–	–QE stop	5 (22 β repeats)	5	MND–HAIRGDTFAT–RAE	a
Triple-mutant Ads								
Ad/ΔF(FG) ΔP-S35-L2	–NCRLNAEKDA–	–TEG----NAV– (Δa.a. 489–492)	–DTTSNPSA–	–QEID stop	35 (6 β repeats)	5	MND–TS---------RAE ΔRGD motif	b
Ad/ΔF(AB) ΔP-S35-L2	–NCSLNGGGDA– (4-a.a. mutation)	–TEGTAYTNAV–	–DTTSNPSA–	–QEID stop	35 (6 β repeats)	5	MND–TS---------RAE ΔRGD motif	b
Triple-mutant Ad containing RGD motif in fiber								
Ad/ΔF(AB) ΔP-S35-RGD-L2	–NCSLNGGGDA– (4-a.a. mutation)	–TEGTAYTNAV–	–DTTSACDCRG DCFCANPSA–	–QEID stop	35 (6 β repeats)	5	MND–TS---------RAE ΔRGD motif	c

[a]See Fig. 1A.

with a four-amino acid mutation of the AB loop (R412S, A415G, E416G, and K417G), the Ad type 35 fiber shaft, and a deletion of the RGD motif of the penton base. Ad/ΔF(FG)ΔP-S35-L2, which is identical to Ad/ΔFΔP-S35-L2 in our previous report (Koizumi *et al.*, 2003a), contains the Ad type 5 fiber knob with a four-amino acid deletion of the FG loop (T489, A490, Y491, and T492), the Ad type 35 fiber shaft, and deletion of the RGD motif of the penton base. Ad/ΔF(AB)ΔP-S35-RGD-L2 contains an RGD motif in the HI loop of the fiber knob in Ad/ΔF(AB)ΔP-S35-L2. Ad-L2 is a conventional Ad vector. All mutations of the mutant Ad vectors and possible interaction of each virus with the cells are summarized in Table 1 and Fig. 1A. All of the mutant Ad vectors used in this study were readily propagated with particle titers similar to that of the conventional Ad vector, Ad-L2 (see Materials and Methods).

To confirm the modification of the fiber protein in each Ad vector, Western blot analysis against fiber protein was performed with rabbit fiber knob polyclonal antibody (Fig. 1B). The mutant fiber and wild-type fiber are easily distinguished because the mutant fiber is smaller than the wild-type fiber because of the small size of the Ad type 35 fiber shaft and because Ad/ΔF(AB)ΔP-S35-L2 has a fiber protein four amino acids longer than that of Ad/ΔF(FG)ΔP-S35-L2. Western blot analysis shows the expected size of the fiber proteins, suggesting that each Ad vector should indeed contain the expected fiber protein.

Gene transfer in vitro

We examined the gene transfer activity in SK HEP-1 cells transduced with Ad/ΔF(AB)ΔP-S35-L2 in comparison with

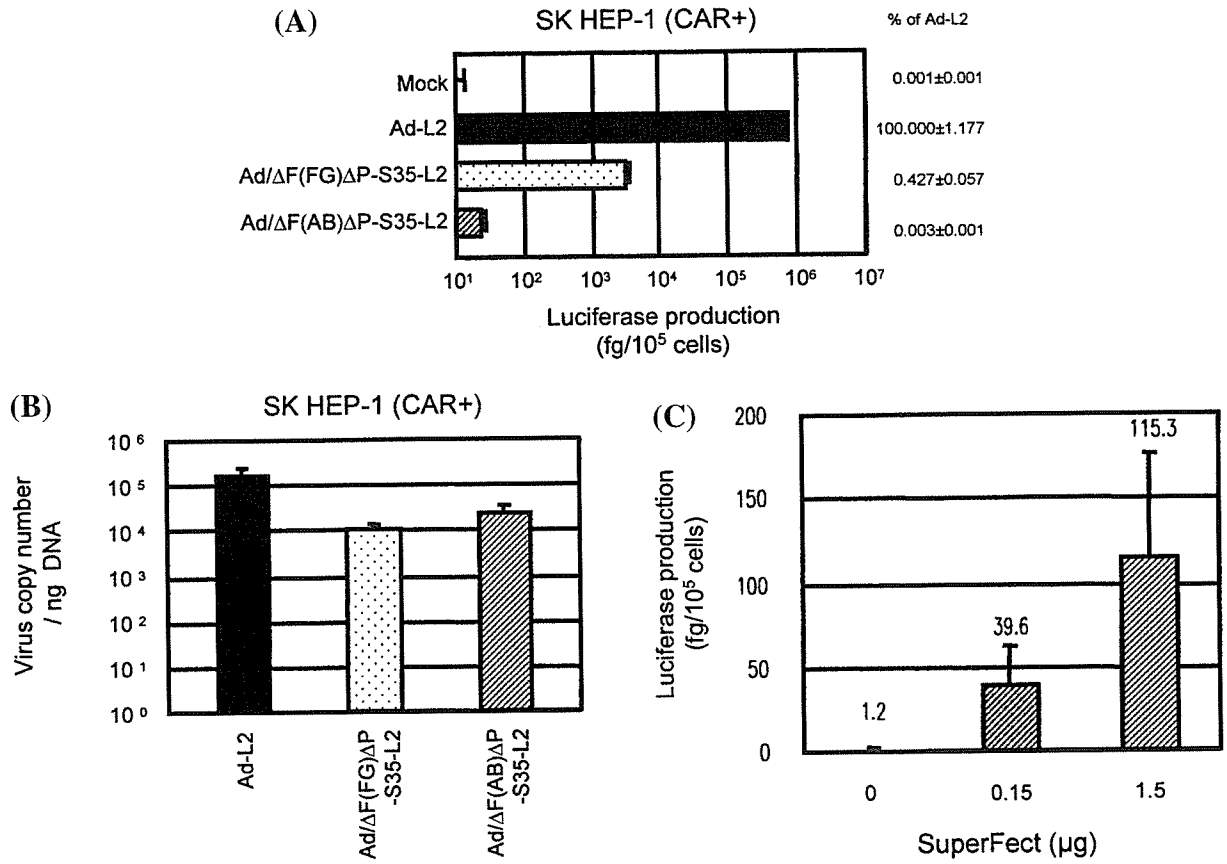

FIG. 2. Luciferase production and viral uptake in SK HEP-1 cells transduced with several Ad vectors. (**A**) Comparison of luciferase production in human cells transduced with Ad-L2, Ad/ΔF(FG)ΔP-S35-L2, or Ad/ΔF(AB)ΔP-S35-L2. SK HEP-1 cells were transduced with Ad-L2, Ad/ΔF(FG)ΔP-S35-L2, or Ad/ΔF(AB)ΔP-S35-L2 (3000 VP/cell) for 1.5 hr. After culture for 48 hr, luciferase production in the cells was measured by luminescence assay. Data are expressed as means ± SD ($n = 4$). Relative levels of luciferase expression are described by designating the value of Ad-L2 as 100. (**B**) Viral uptake in SK HEP-1 cells. SK HEP-1 cells were transduced with Ad-L2, Ad/ΔF(FG)ΔP-S35-L2, or Ad/ΔF(AB)ΔP-S35-L2 at 3000 VP/cell. After culture for 1.5 hr, the cells were washed with PBS, resuspended in 0.05% trypsin–0.5 m*M* EDTA–PBS solution, and incubated at 37°C for 10 min. After this incubation, the cells were incubated at 37°C for 10 min with 0.05% DNase I–0.5 *M* $MgCl_2$–PBS, washed with PBS, and resuspended in 0.1 *M* EDTA–PBS solution. The amounts of Ad genome DNA isolated from the cells were quantified with the TaqMan fluorogenic detection system. Data are expressed as means ± SD ($n = 4$). (**C**) Comparison of luciferase production in SK HEP-1 cells transduced with a complex of Ad/ΔF(AB)ΔP-S35-L2 and SuperFect. SK HEP-1 cells (2×10^4 cells) were seeded into a 24-well dish. The next day, the cells were either not transduced or were transduced with a complex of Ad/ΔF(AB)ΔP-S35-L2 and SuperFect (0.15 or 1.5 μg) (Qiagen) for 1.5 hr. After culture for 48 hr, luciferase production in the cells was measured with a luciferase assay system. Data are expressed as means ± SD ($n = 4$).

Ad/ΔF(FG)ΔP-S35-L2 or Ad-L2 (Fig. 2). SK HEP-1 cells express both CAR and α_v integrin (Koizumi *et al.*, 2001, 2003b). To measure the internalization of Ad particles into the cells, Ad genome DNA in the cells after 1.5 hr of transduction with each Ad vector was also quantified with the TaqMan fluorogenic detection system. Viral particles associated with the cellular surface were removed by trypsin–EDTA–PBS and DNase I–$MgCl_2$–PBS treatment as described in Materials and Methods. Cells transduced with Ad/ΔF(AB)ΔP-S35-L2 showed much lower luciferase production than those transduced with Ad/ΔF(FG)ΔP-S35-L2. Ad/ΔF(AB)ΔP-S35-L2 mediated only approximately 0.003% of the luciferase production of Ad-L2, whereas Ad/ΔF(FG)ΔP-S35-L2 mediated approximately 0.42% of that of Ad-L2 (Fig. 2A). In contrast, the amounts of Ad/ΔF(AB)ΔP-S35-L2 DNA and Ad/ΔF(FG)ΔP-S35-L2 DNA in SK HEP-1 cells were only 10-fold lower than those of Ad-L2 DNA. The amounts of Ad/ΔF(AB)ΔP-S35-L2 DNA in the cells were similar to those of Ad/ΔF(FG)ΔP-S35-L2 DNA (Fig. 2B).

Because Ad/ΔF(AB)ΔP-S35-L2 showed extremely low transduction activity, we examined luciferase production in SK HEP-1 cells transduced with Ad/ΔF(AB)ΔP-S35-L2 in the presence of SuperFect (polyamidoamine dendrimer reagent; Qiagen). Ad/ΔF(AB)ΔP-S35-L2 mediated high levels of luciferase production in a dose-dependent manner with SuperFect (Fig. 2C). Therefore, low luciferase production by Ad/ΔF(AB)ΔP-S35-L2 is likely due to a lack of specific binding activity between the virus and target cells and to endosomal escape, but it was not due to the virus being defective. These results suggest that the abolishment of CAR, integrin, and HSG binding of Ad vectors significantly reduces transduction efficiency and that the four-amino acid mutation of the AB loop of the fiber knob reduces transduction to a greater extent than does the four-amino acid deletion of the FG loop of the fiber knob.

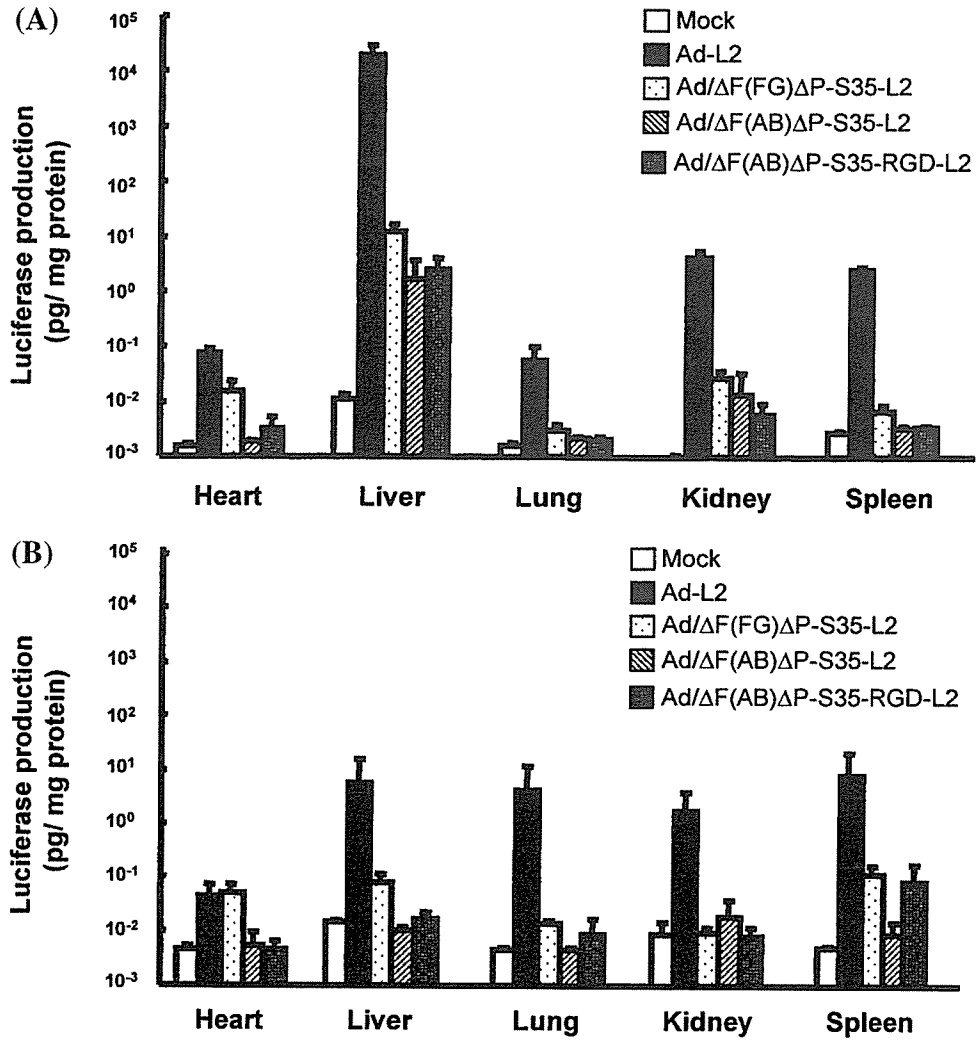

FIG. 3. Luciferase production in mice after systemic administration of Ad-L2, Ad/ΔF(FG)ΔP-S35-L2, or Ad/ΔF(AB)ΔP-S35-L2, or Ad/ΔF(AB)ΔP-S35-RGD-L2. Ad-L2, Ad/ΔF(FG)ΔP-S35-L2, Ad/ΔF(AB)ΔP-S35-L2, or Ad/ΔF(AB)ΔP-S35-RGD-L2 was (**A**) intravenously (3.0×10^{10} VP) or (**B**) intraperitoneally (1.0×10^{11} VP) injected into mice. Forty-eight hours later, the heart, lung, liver, kidney, and spleen were harvested and luciferase production was measured by a luciferase assay system. All data represent the means ± SD of four to six mice.

Gene transfer in vivo

Next, to examine whether natural Ad tropism to tissues, including liver, can be more suppressed by Ad/ΔF(AB)ΔP-S35-L2 in comparison with Ad/ΔF(FG)ΔP-S35-L2, each Ad vector was administered to mice by either intravenous (3.0×10^{10} VP) or intraperitoneal (1.0×10^{11} VP) injection, and luciferase production in the organ was measured (Figs. 3 and 4). In the case of intraperitoneal injection, a high dose of Ad vector (1.0×10^{11} VP) was injected because luciferase production was not detected in mouse tissue after intraperitoneal injection of 3.0×10^{10} VP of either Ad/ΔF(FG)ΔP-S35-L2 or Ad/ΔF(AB)ΔP-S35-L2. With intravenous injection, Ad/ΔF(AB)ΔP-S35-L2 mediated approximately 15,000-fold lower liver transduction than Ad-L2, and resulted in approximately 10-fold lower liver transduction compared with Ad/ΔF(FG)ΔP-S35-L2 (Fig. 3A). A similar pattern was observed in the heart, lung, kidney, and spleen, although the absolute levels of luciferase production were much lower compared with those in the liver.

With intraperitoneal injection, Ad-L2 mediated similar levels of luciferase production in the liver, lung, kidney, and spleen (Fig. 3B). The suppressive pattern of luciferase production in each organ after intraperitoneal injection of Ad/ΔF(AB)ΔP-S35-L2 and Ad/ΔF(FG)ΔP-S35-L2 was similar to that after intravenous injection. Ad/ΔF(AB)ΔP-S35-L2 showed much more reduced luciferase production in the organs than did Ad/ΔF(FG)ΔP-S35-L2 (Fig. 3B). Luciferase production in each organ after intraperitoneal injection of Ad/ΔF(AB)ΔP-S35-L2 was at almost background levels. These results indicate that the triple-mutant Ad vector containing a mutation of the AB loop of the fiber knob exhibits much lower luciferase production than does the triple-mutant Ad vector containing a mutation of the FG loop of the fiber knob, in both intravenously and intraperitoneally injected mice.

Distribution of Ad vectors after systemic administration

To examine the biodistribution of Ad/ΔF(AB)ΔP-S35-L2, Ad/ΔF(FG)ΔP-S35-L2, and Ad-L2 in mice at a early stage after intravenous (3×10^{10} VP) and intraperitoneal (1×10^{11} VP) injection, the amounts of Ad DNA in organs 3 hr after Ad vector injection were measured with the TaqMan fluorogenic detection system. The amounts of Ad DNA in organs after intravenous injection showed no significant difference among mice injected with Ad/ΔF(AB)ΔP-S35-L2, Ad/ΔF(FG)ΔP-S35-L2, or Ad-L2 (Fig. 4A), although the amounts of Ad/ΔF(AB)ΔP-S35-L2 and Ad/ΔF(FG)ΔP-S35-L2 in the kidney were less than that of Ad-L2. In the case of intraperitoneal injection, Ad/ΔF(AB)ΔP-S35-L2 and Ad/ΔF(FG)ΔP-S35-L2 showed higher or similar amounts of Ad DNA in the liver or spleen, respectively, than Ad-L2 (Fig. 4B).

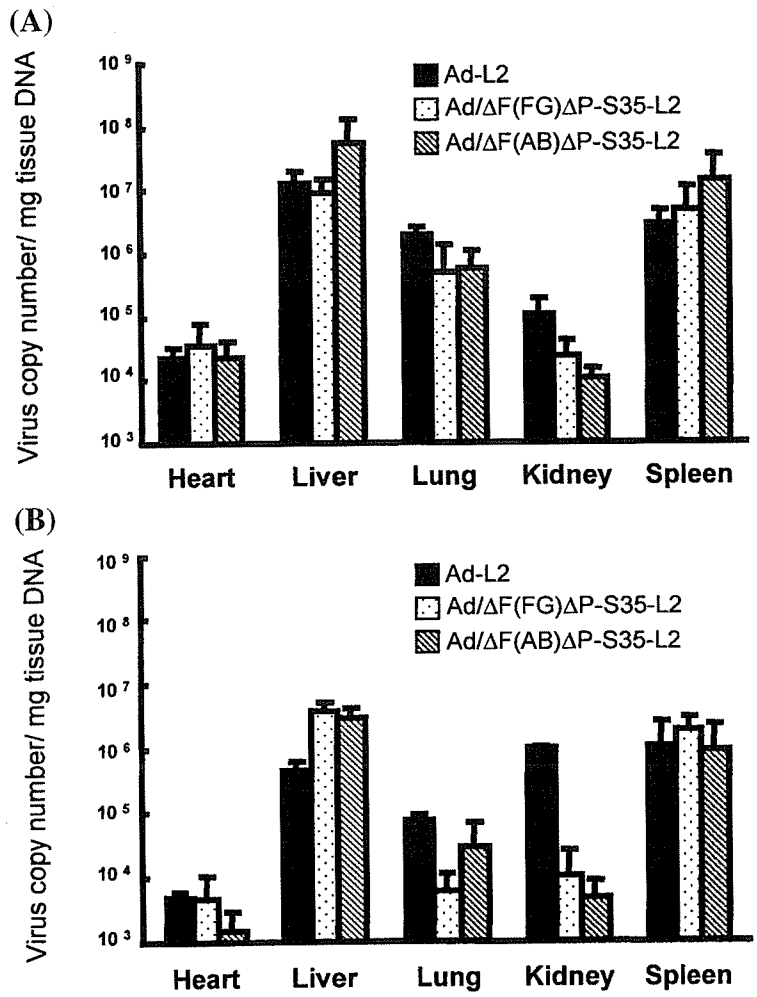

FIG. 4. Biodistribution of viral DNA after systemic administration of Ad-L2, Ad/ΔF(FG)ΔP-S35-L2, or Ad/ΔF(AB)ΔP-S35-L2 into mice. Ad-L2, Ad/ΔF(FG)ΔP-S35-L2, or Ad/ΔF(AB)ΔP-S35-L2 was (**A**) intravenously (3.0×10^{10} VP) or (**B**) intraperitoneally (1.0×10^{11} VP) injected into mice. Three hours later, the heart, lung, liver, kidney, and spleen were harvested and Ad vector DNA was measured with the quantitative TaqMan PCR assay. All data represent the means ± SD of four to six mice.

Less Ad/ΔF(AB)ΔP-S35-L2 accumulated in the heart, lung, and kidney compared with Ad-L2. The data regarding luciferase production (Fig. 3) and the amounts of Ad DNA in most organs, especially the liver (Fig. 4), showed discrepancies in the cases of both intravenous and intraperitoneal injection.

Amounts of Ad vector DNA in liver parenchymal and nonparenchymal cells

Next, to examine why there is an especially large difference between luciferase production and Ad DNA accumulation in the liver, the amounts of Ad/ΔF(AB)ΔP-S35-L2, Ad/ΔF(FG)ΔP-S35-L2, and Ad-L2 delivered to parenchymal cells (PCs; hepatocyte) and nonparenchymal cells (NPCs; Kupffer cells and endothelial cells) 3 hr after injection were measured with the TaqMan fluorogenic detection system (Fig. 5). In the case of intravenous injection of Ad vector at 3×10^{10} VP, more Ad-L2 DNA was found in PCs than in NPCs, whereas there was less Ad/ΔF(AB)ΔP-S35-L2 and Ad/ΔF(FG)ΔP-S35-L2 DNA in PCs than in NPCs (Fig. 5A). This finding is consistent with our previous reports based on analysis by semiquantitative PCR (Koizumi *et al.*, 2003a). In the case of intraperitoneal injection of Ad vector at 1×10^{11} VP, Ad/ΔF(AB)ΔP-S35-L2, Ad/ΔF(FG)ΔP-S35-L2, and Ad-L2 DNA accumulated more in NPCs than in PCs (Fig. 5B). Thus, lower luciferase production in the liver after intravenous and intraperitoneal injection of Ad/ΔF(AB)ΔP-S35-L2 and Ad/ΔF(FG)ΔP-S35-L2 would be partly due to higher accumulation of vectors in NPCs. The NPCs might take up Ad via phagocytosis and resolve viral DNA, resulting in lower gene expression.

Blood clearance of Ad vectors

To examine the biodistribution in more detail, the blood clearance rates of Ad/ΔF(AB)ΔP-S35-L2, Ad/ΔF(FG)ΔP-S35-L2, and Ad-L2 in mice were measured with the TaqMan fluorogenic detection system (Fig. 6). In the case of intravenous injection, blood clearance curves for Ad/ΔF(AB)ΔP-S35-L2, Ad/ΔF(FG)ΔP-S35-L2, and Ad-L2 were similar, and all the vectors showed rapid decrease from the bloodstream (Fig. 6A). In the case of intraperitoneal injection, Ad/ΔF(AB)ΔP-S35-L2 and Ad/ΔF(FG)ΔP-S35-L2 showed similar blood clearance curves. The amounts of Ad/ΔF(AB)ΔP-S35-L2 and Ad/ΔF(FG)ΔP-S35-L2 DNA were approximately 10-fold higher than those of Ad-L2 DNA between 60 and 120 min after injection (Fig. 6B). The area under the curve (AUC_{2-180}) values of Ad/ΔF(AB)ΔP-S35-L2 and Ad/ΔF(FG)ΔP-S35-L2 were 5- to 7-fold higher than that of Ad-L2 (data not shown). Higher levels of Ad/ΔF(AB)ΔP-S35-L2 and Ad/ΔF(FG)ΔP-S35-L2 were found to be introduced into the bloodstream from the intraperitoneum than Ad-L2.

Liver serum enzymes and serum interleukin-6 levels after administration of Ad vector

Systemic administration of Ad vectors results in the initiation of inflammation and strong innate immunity responses in animals and humans (Schnell *et al.*, 2001; Muruve, 2004), and this toxicity limits the utility of Ad vectors for gene therapy. To evaluate the toxicity of each Ad vector, we measured the levels of AST, ALT, and IL-6 in serum after systemic administration. After injection of Ad/ΔF(AB)ΔP-S35-L2 and Ad/ΔF(FG)ΔP-S35-L2 in mice (both by intravenous and intraperitoneal injection), the levels of AST and ALT in serum were similar to those in nontreated mice, suggesting that Ad/ΔF(AB)ΔP-S35-L2 and Ad/ΔF(FG)ΔP-S35-L2 did not show liver toxicity (Fig. 7). In contrast, Ad-L2 led to high levels of AST and ALT in serum after intravenous injection (Fig. 7A). In the case of IL-6, neither intravenous nor intraperitoneal injection of Ad/ΔF(AB)ΔP-S35-L2 or Ad/ΔF(FG)ΔP-S35-L2 mediated IL-6 production, whereas injection of Ad-L2 led to high levels of IL-6 in serum (Fig. 8). These results suggest that Ad/ΔF(AB)ΔP-S35-L2 and Ad/ΔF(FG)ΔP-S35-L2 show less liver toxicity and innate immunity reaction (IL-6 production) after systemic administration.

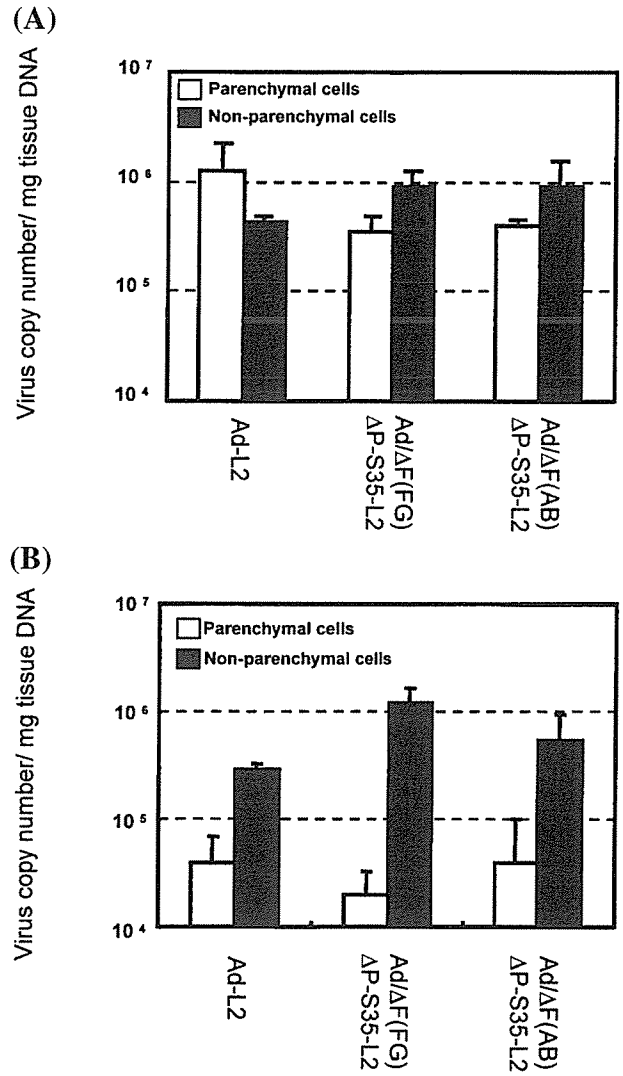

FIG. 5. Biodistribution of viral DNA in liver parenchymal and nonparenchymal cells. Ad-L2, Ad/ΔF(FG)ΔP-S35-L2, or Ad/ΔF(AB)ΔP-S35-L2 was (**A**) intravenously (3.0×10^{10} VP) or (**B**) intraperitoneally (1.0×10^{11} VP) injected into mice. Collagenase perfusion was performed 3 hr after injection of Ad vector to separate liver PCs and NPCs. Total DNA, including Ad vector DNA, was isolated from the cells, and Ad vector DNA was measured by quantitative TaqMan PCR assay. All data represent the means ± SD of four to six mice.

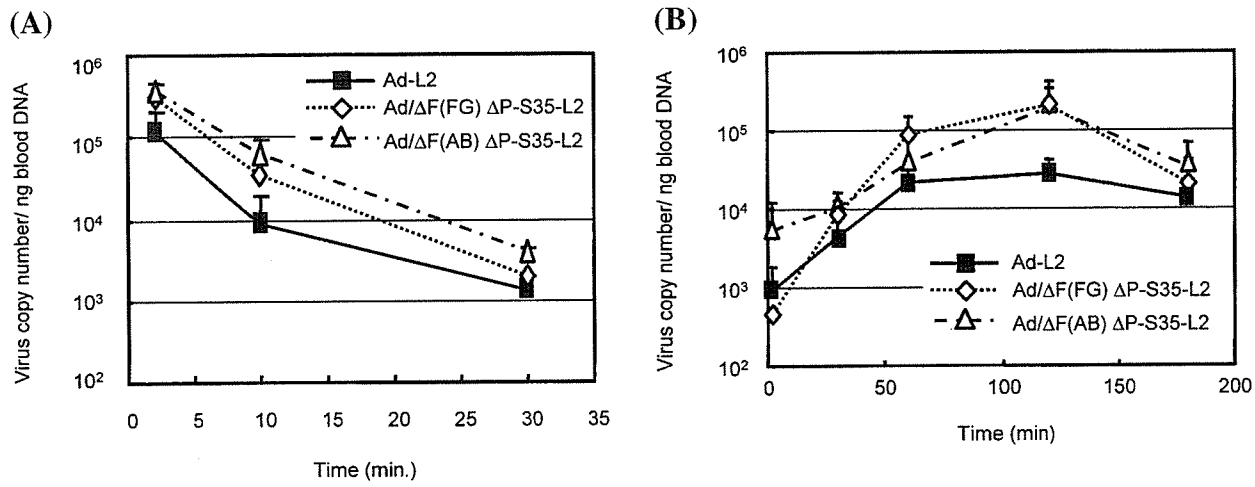

FIG. 6. Blood clearance of Ad-L2, Ad/ΔF(FG)ΔP-S35-L2, and Ad/ΔF(AB)ΔP-S35-L2 after systemic administration into mice. Ad-L2, Ad/ΔF(FG)ΔP-S35-L2, or Ad/ΔF(AB)ΔP-S35-L2 was (**A**) intravenously (3.0×10^{10} VP) or (**B**) intraperitoneally (1.0×10^{11} VP) injected, and blood was drawn by retroorbital bleeding at the indicated times postinjection. Total DNA, including Ad vector DNA, was isolated from the blood, and Ad vector DNA was measured by quantitative TaqMan PCR assay. All data represent the means ± SD of four to six mice.

Inclusion of RGD ligand into the fiber knob in triple-mutant Ad vectors

For the development of a targeted Ad vector, addition of foreign ligands into a viral capsid that no longer infects cells is required. For this purpose, Ad/ΔF(AB)ΔP-S35-RGD-L2, in which the RGD peptide was introduced into the HI loop of the fiber knob of Ad/ΔF(AB)ΔP-S35-L2, was constructed, and gene transfer activity was measured in SK HEP-1 cells (Fig. 9A). Ad/ΔF(AB)ΔP-S35-RGD-L2 showed 100-fold higher luciferase production in SK HEP-1 cells than did Ad/ΔF(AB)ΔP-S35-L2 (Fig. 9A). In the inhibition experiment using RGD peptide, luciferase production in cells transduced with Ad/ΔF(AB)ΔP-S35-RGD-L2 was suppressed by RGD peptide in a dose-dependent fashion, suggesting that Ad/ΔF(AB)ΔP-S35-RGD-L2 mediates gene transfer through RGD peptides in the fiber knob (Fig. 9B).

Next, to examine whether Ad/ΔF(AB)ΔP-S35-RGD-L2 mediates luciferase production *in vivo* in a manner different from Ad/ΔF(AB)ΔP-S35-L2, Ad/ΔF(AB)ΔP-S35-RGD-L2 was administered to mice by either intravenous (3.0×10^{10} VP) or intraperitoneal (1.0×10^{11} VP) injection, and luciferase production in organs was measured (Fig. 3). Data suggest that addition of RGD peptide to the triple-mutant Ad vector does not change the biodistribution *in vivo*, although intraperitoneal injection of Ad/ΔF(AB)ΔP-S35-RGD-L2 mediated slightly higher luciferase production in the spleen compared with Ad/ΔF(AB)ΔP-S35-L2.

DISCUSSION

In this study, we generated a new Ad vector with a four-amino acid mutation of the AB loop in the fiber knob (T489, A490, Y491, and T492), deletion of the RGD motif of the penton base, and substitution of the fiber shaft domain for that derived from Ad type 35, and demonstrated that this triple-mutant Ad vector shows significantly lower gene transfer activity (both *in vitro* and *in vivo*). The triple-mutant Ad vector containing a mutation of the AB loop in the fiber knob mediated much lower gene transfer activity than the previously generated triple-mutant Ad vector containing a mutation of the FG loop in the fiber knob (Koizumi *et al.*, 2003a). Furthermore, the triple-mutant Ad vector was less toxic, and showed almost background levels of both liver serum enzymes (AST and ALT) and IL-6 in mouse serum.

Ad vectors show nonspecific tissue distribution after *in vivo* gene transfer. This distribution is due largely to the relatively broad expression of CAR, α_v integrin, and HSGs; the size of sinusoidal fenestrae (Fechner *et al.*, 1999; Lievens *et al.*, 2004); and the complement system (Zinn *et al.*, 2004). To generate targeted Ad vectors, several groups have reported CAR binding-ablated Ad vectors with an AB or FG loop mutation of the fiber knob (Bewley *et al.*, 1999; Kirby *et al.*, 1999; Asaoka *et al.*, 2000; Alemany and Curiel, 2001; Einfeld *et al.*, 2001; Leissner *et al.*, 2001; Mizuguchi *et al.*, 2002; Smith *et al.*, 2002). However, there has been no report on the difference in gene transfer activity (*in vitro* and *in vivo*) between Ad vectors with an AB loop mutation and those with an FG loop mutation. The present study shows that mutation of the AB loop in the fiber knob is better than deletion of the FG loop for lowering transgene expression, at least with the triple-mutant Ad vector. Cells transduced with Ad/ΔF(AB)ΔP-S35-L2 or Ad/ΔF(FG)ΔP-S35-L2 produced luciferase at rates of only 0.003 and 0.42%, respectively, relative to the rate of luciferase production in cells transduced with Ad-L2 (Fig. 2A). The FG loop mutation in the fiber knob might continue to facilitate a weak interaction between CAR and the fiber knob. One of the interesting findings is that the amounts of Ad/ΔF(AB)ΔP-S35-L2 DNA and Ad/ΔF(FG)ΔP-S35-L2 DNA in the cells were only 10-fold lower than those of Ad-L2 DNA, even after the cells were treated with trypsin–EDTA and DNase I (Fig. 2B). Therefore, the cells would take up considerable amounts of Ad/ΔF(AB)ΔP-S35-L2 and Ad/ΔF(FG)ΔP-S35-L2 nonspecifically, although neither vector mediated luciferase production.

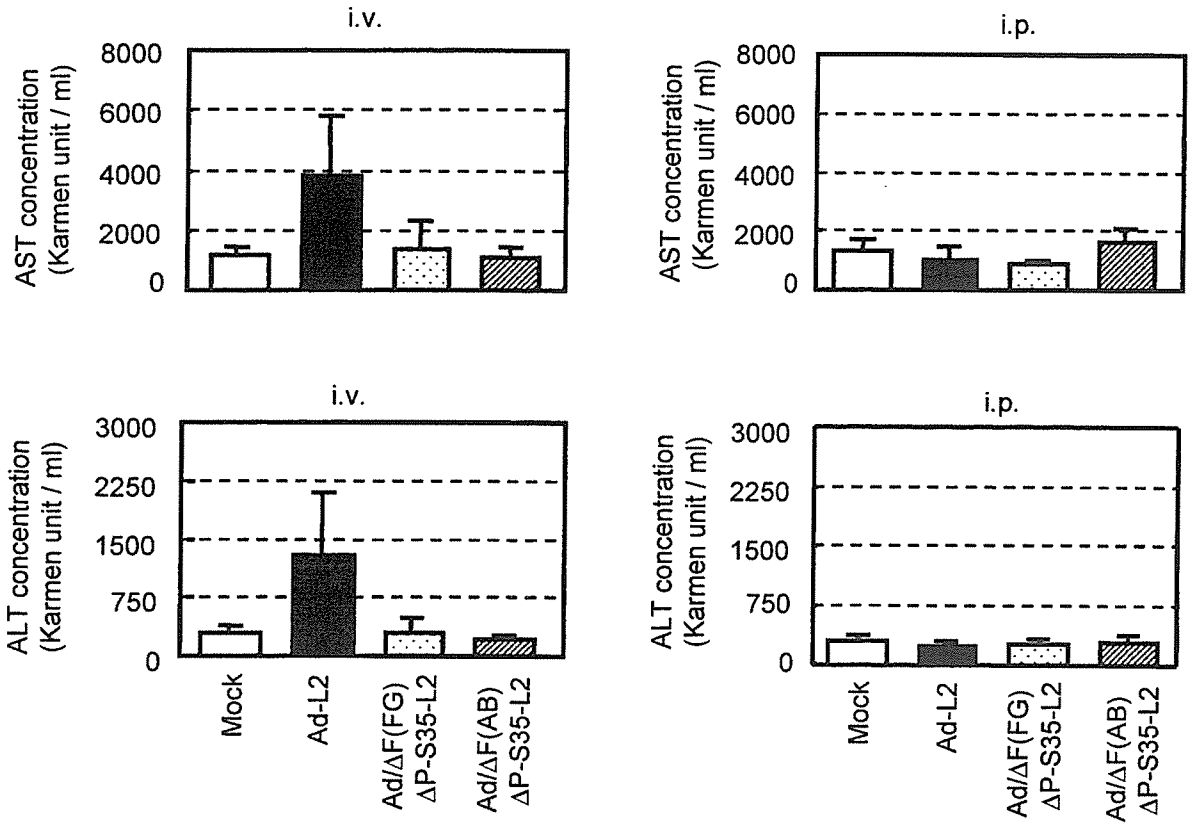

FIG. 7. Serum enzymes levels after systemic administration of Ad-L2, Ad/ΔF(FG)ΔP-S35-L2, or Ad/ΔF(AB)ΔP-S35-L2 into mice. Blood samples were collected from the inferior vena cava 48 hr after intravenous (3.0×10^{11} VP) or intraperitoneal (1.0×10^{11} VP) injection of Ad-L2, Ad/ΔF(FG)ΔP-S35-L2, or Ad/ΔF(AB)ΔP-S35-L2. Serum samples were collected into separate tubes containing no anticoagulant for coagulation, and aspartate aminotransferase (AST) and alanine aminotransferase (ALT) levels in serum were measured with a Transaminase-CII kit. All data represent the means ± SD of four mice.

We demonstrated that the newer triple-mutant Ad vector containing a mutation of the AB loop mediates approximately 15,000- and 500-fold lower mouse liver transduction by intravenous and intraperitoneal injection, respectively, than the conventional Ad vector (Fig. 3). However, the amounts of triple-mutant Ad vector DNA in the liver after intravenous or intraperitoneal injection were similar to or higher than those with the conventional Ad vector (Fig. 4). The difference between luciferase production and Ad DNA accumulation in the liver would be due to higher accumulation of triple-mutant Ad vector DNA in the NPCs (Kupffer cells and endothelial cells) (Fig. 5) as well as to nonspecific viral uptake in the liver. Because higher amounts of the triple-mutant Ad vector were taken up nonspecifically into the cultured cells (Fig. 2B), the liver cells *in vivo* would also take up large amounts of virus nonspecifically. Our previous report showed that most Ad DNA (especially the triple-mutant Ad DNA) taken up in NPCs disappears 48 hr after intravenous administration (Koizumi *et al.*, 2003a). Triple-mutant Ad vectors in NPCs might be resolved, resulting in significantly lower gene expression in the liver. Furthermore, Miyazawa *et al.* have reported that exchanging the Ad type 5 fiber (subgroup C) for the Ad type 7 fiber (subgroup B) on an Ad type 5 capsid resulted in altered cellular trafficking compared with parental Ad type 5 (Miyazawa *et al.*, 1999, 2001). Therefore, even if the triple-mutant Ad vector, in which the Ad type 5 fiber shaft was exchanged for the Ad type 35 fiber shaft (subgroup B), was taken up into cells, it might have defects in viral escape from the endosome to the cytoplasm (Nicklin *et al.*, 2005).

We and others have reported that the conventional Ad vector has a half-life in the bloodstream of approximately 2 min after intravenous injection (Alemany *et al.*, 2000; Alemany and Curiel, 2001; Koizumi *et al.*, 2003a; Sakurai *et al.*, 2003). The triple-mutant Ad vector and the conventional Ad vector presented similar clearance kinetics from the circulation after intravenous injection (Fig. 6A). In the case of intraperitoneal injection, the AUC_{2-180} value of the triple-mutant Ad vector in the bloodstream was approximately five to seven times higher than that of the conventional Ad vector (Fig. 6B). It remains unclear why intraperitoneally injected vectors persist longer in the blood (Akiyama *et al.*, 2004). The vector might associate with blood factors or cells (Shayakhmetov *et al.*, 2005). It was also found that intraperitoneally injected vectors accumulated more in NPCs than in PCs (Fig. 5B). This NPC-mediated uptake might be an obstacle for the targeted Ad vector when it is intraperitoneally injected. Because the present vector has no targeted ligands, more detailed studies should be done after high-affinity ligands are displayed on the vectors. If high levels of NPC-mediated uptake were avoided by the addition of ligands,

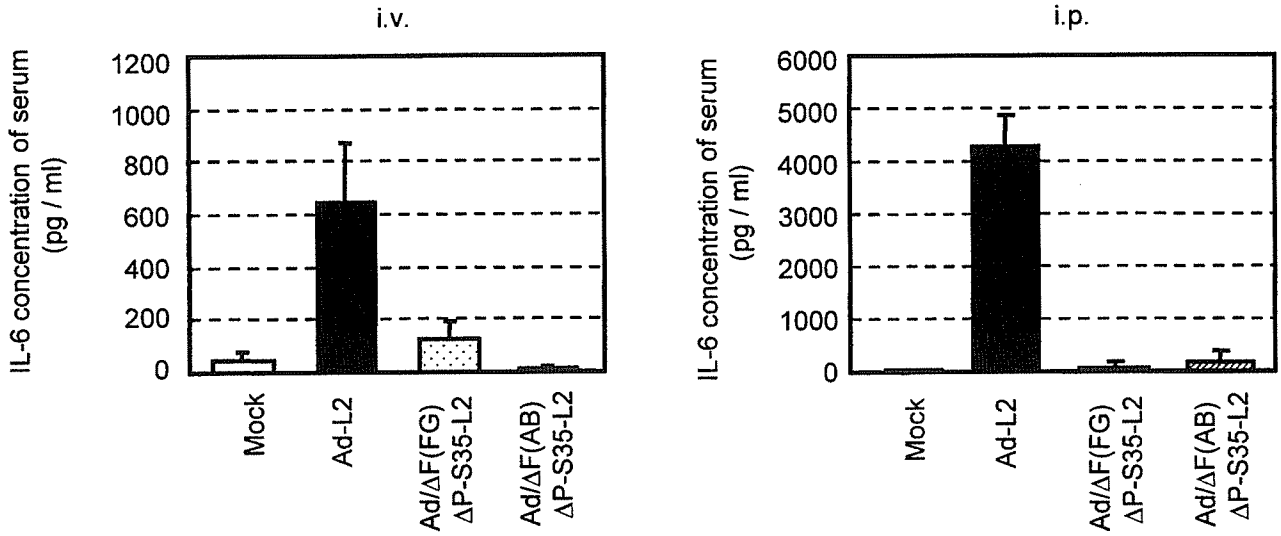

FIG. 8. Interleukin (IL)-6 levels in serum after systemic administration of Ad-L2, Ad/ΔF(FG)ΔP-S35-L2, or Ad/ΔF(AB)ΔP-S35-L2 into mice. Blood samples were collected from the inferior vena cava 3 hr after intravenous (3.0×10^{11} VP) or intraperitoneal (1.0×10^{11} VP) injection of Ad-L2, Ad/ΔF(FG)ΔP-S35-L2, or Ad/ΔF(AB)ΔP-S35-L2. Serum samples were collected into separate tubes containing no anticoagulant for coagulation, and IL-6 levels in the serum were measured by ELISA. All data represent the means ± SD of six mice.

the increased persistence of the vector in the blood in the case of intraperitoneal injection might give us a way to overcome obstacles to the development of targeted Ad vectors.

In the *in vivo* viral uptake experiment, the yield of viral DNA from total liver (Fig. 4) was an order of magnitude more than the total yield obtained from PCs and NPCs (Fig. 5). We speculated that extracellular virus, which would be present in the yield obtained from total liver but not in the yield obtained from fractionated cells, might be involved, because extracellular virus would be moved by collagenase treatment into the fractionated cells. To demonstrate this, we examined the effect of collagenase or trypsin treatment on the amounts of viral DNA in cultured cells. SK HEP-1 cells were transduced with Ad-L2 or Ad/ΔF(AB)ΔP-S35-L2 (3000 VP/cell). After a 3-hr culture period, the cells were washed with PBS, collagenase (0.01%), or trypsin (0.025%). The amounts of Ad genomic DNA in cells were

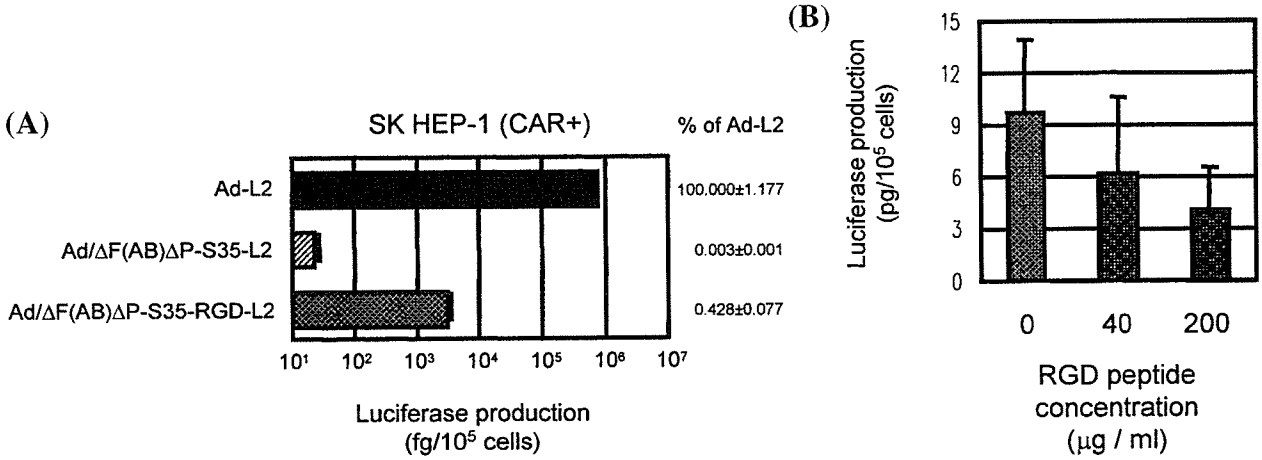

FIG. 9. Luciferase production in human cells transduced with Ad vectors containing RGD motif in the fiber knob. (**A**) Comparison of luciferase production in human cells transduced with Ad-L2, Ad/ΔF(AB)ΔP-S35-L2, or Ad/ΔF(AB)ΔP-S35-RGD-L2. SK HEP-1 cells were transduced with 3000 VP/cell of Ad-L2, Ad/ΔF(AB)ΔP-S35-L2, or Ad/ΔF(AB)ΔP-S35-RGD-L2 for 1.5 hr. After culture for 48 hr, luciferase production in the cells was measured by a luciferase assay system. The data are expressed as means ± SD ($n = 4$). The relative expression levels are described by designating the value of Ad-L2 as 100. (**B**) Effects of RGD peptide on the transduction efficiency of Ad/ΔF(AB)ΔP-S35-RGD-L2 into SK HEP-1 cells. SK HEP-1 cells were preincubated with RGD peptide (0, 1.6, 8, or 40 μg/ml) for 10 min. The cells were then transduced with 300 VP/cell of Ad/ΔF(AB)ΔP-S35-RGD-L2 for 0.5 hr in the presence of RGD peptide. After culture for 48 hr, luciferase production was measured by a luciferase assay system. The data are expressed as means ± SD ($n = 6$).

quantified with the TaqMan fluorogenic detection system. Data showed that collagenase or trypsin treatment decreased 2- to 3.5-fold the amounts of Ad DNA in cells (data not shown), suggesting that nonspecific viral association would lead to the overestimation of viral uptake by the cells. Therefore, the difference in the yields between Figs. 4 and 5 would be reasonable.

The initiation of inflammation and strong innate immunity responses occur after systemic administration of Ad vectors to animals and humans, and this toxicity limits the utility of Ad vectors for gene therapy (Muruve, 2004). Increased cytokine production after injection of Ad vectors was reported to be due to the introduction of input Ad vectors to Kupffer cells in the liver and dendritic cells (Lieber *et al.*, 1997; Schnell *et al.*, 2001; Morral *et al.*, 2002; Reid *et al.*, 2002; Philpott *et al.*, 2004). Lieber *et al.* have reported that IL-6 production in mice after injection of Ad vectors was decreased by preinjection of $GaCl_2$, which can decrease the levels of Kupffer cells in mouse liver (Lieber *et al.*, 1997). On the other hand, Muruve reported that Kupffer cells avidly take up systemically administered Ad vectors, but the blockade of Kupffer cells has minimal impact on the innate immune response in the liver (Muruve, 2004). Although our experiment showed that large amounts of the triple-mutant Ad vector accumulated in the NPC fraction, which contains Kupffer cells and liver sinusoidal (endothelial) cells, IL-6 was not produced in mice after injection of the triple-mutant Ad vector (Fig. 8). Therefore, Ad vectors would be capable of inducing IL-6 production in cells other than Kupffer cells. De Geest *et al.* reported that the spleen, not the liver, is the major site of IL-6 production after Ad vector transfer (De Geest *et al.* 2005), although in the present study the triple-mutant Ad vector accumulated in the spleen as much as did the conventional Ad vector (Fig. 4). There are several possible reasons why the triple-mutant Ad vector does not mediate IL-6 production *in vivo*. Philpott *et al.* have reported that maturation of dendritic cells, which are IL-6-producing cells, by infection with Ad vectors requires the RGD motif of the Ad penton base (Philpott *et al.*, 2004). The triple-mutant Ad vector without the RGD motif in the penton base would interact differently with IL-6-producing cells than would the conventional Ad vector. Liu *et al.* have reported that conventional Ad vectors are delivered into liver sinusoid cells as well as Kupffer cells after systemic injection (Liu *et al.*, 2003). Schiedner *et al.* have reported that Ad vectors activate liver endothelial cells after infection of Kupffer cells (Schiedner *et al.*, 2003). The difference in distribution between the triple-mutant Ad vector and the conventional Ad vector in liver sinusoid and Kupffer cells may contribute to IL-6 production. Furthermore, Zsengeller *et al.* demonstrated that Ad vector internalization and endosomal escape were required for cytokine induction in alveolar macrophages (Zsengeller *et al.*, 2000). The triple-mutant Ad vector might have reduced the level of endosomal escape in comparison with the conventional Ad vector. Specific viral component(s) of the Ad vector, viral distribution in the specific cell types, and/or viral distribution in the cellular compartment might determine IL-6 production. Elucidation of a mechanism for innate immune responses after administration of Ad vectors might be obtained by investigating the precise distribution of the triple-mutant Ad vector after systemic administration.

Finally, regarding the feasibility of using triple-mutant Ad vectors as targeted vectors, we constructed triple-mutant Ad vectors containing the RGD motif, which has high affinity for α_v integrins, in the HI loop of the fiber knob. This triple-mutant Ad vector with the RGD motif was found to show efficient *in vitro* gene transfer through RGD peptides in the fiber knob (Fig. 9). We also examined *in vivo* luciferase production and serum levels of AST, ALT, and IL-6 in mice after administration of this RGD motif-containing vector. However, the patterns of luciferase production *in vivo* (Fig. 3) and the serum levels of AST, ALT, and IL-6 (data not shown) postadministration were similar to those produced with the triple-mutant Ad vector without any ligands. Because the RGD peptide used in the present study was first isolated from a phage display library and used to "home" to endothelial cells in tumor tissue (Koivunen *et al.*, 1995; Pasqualini *et al.*, 1997), and because the endothelial cells in normal tissue do not express higher levels of α_v integrin than are found in tumor tissue, the RGD motif may not be the optimal peptide for increasing *in vivo* transduction efficiency after systemic injection. Another possible reason why this RGD motif-containing vector did not increase transduction *in vivo* is that the affinity of the introduced RGD peptides for integrin might be weak compared with the knob–CAR interaction. Furthermore, fiber mutation might affect encapsidation, stability, and flexibility of the vector. The resultant subtle alteration in fiber biology might negatively affect the transduction efficiency of this vector. Altered fiber biology might also be involved in the lower gene transduction efficiency of the triple-mutant Ad vector.

For the development of targeted Ad vectors, incorporation of a foreign ligand (i.e., peptide), one with high affinity for a specific cellular receptor, into the capsids of Ad vectors will also be required. The triple-mutant Ad vector was designed to have unique restriction sites (*Csp*45I or *Cla*I) in both the HI loop and the C-terminal coding region of the fiber knob (Mizuguchi *et al.*, 2001; Koizumi *et al.*, 2001, 2003b). Therefore, any targeting ligand can be easily displayed in the fiber knob of the triple-mutant Ad vector by cloning its gene into either of these regions, using simple *in vitro* ligation.

In summary, we have further improved the triple-mutant Ad vector by ablating CAR, α_v integrin, and HSG binding by introducing a mutation of the AB loop into the fiber knob (R412S, A415G, E416G, and K417G). This vector was found to mediate significantly lower tissue transduction both *in vitro* and *in vivo* (intravenous and intraperitoneal injection). Furthermore, we showed that this triple-mutant Ad vector reduces (or blunts) liver toxicity and innate immunity responses (IL-6 production). Inclusion of the RGD peptide in the HI loop of the fiber knob of the triple-mutant Ad vector restored gene transfer activity. Thus, the newer triple-mutant Ad vector will likely be a fundamental vector for targeted gene delivery.

ACKNOWLEDGMENTS

The authors thank Tomomi Sasaki and Takashi Fukushima for technical assistance. This work was supported by grants from the Ministry of Health, Labor, and Welfare of Japan and a Grant-in-Aid for Scientific Research in Priority Areas from the Ministry of Education, Culture, Sports, Science, and Technology (MEXT) of Japan. T.H. is the recipient of a fellowship from the Japan Society for the Promotion of Science.

REFERENCES

AKIYAMA, M., THORNE, S., KIRN, D., ROELVINK, P., EINFELD, D., KING, C., and WICKHAM, T. (2004). Ablating CAR and integrin binding in adenovirus vectors reduces nontarget organ transduction and permits sustained bloodstream persistence following intraperitoneal administration. Mol. Ther. **9,** 218–230.

ALEMANY, R., and CURIEL, D.T. (2001). CAR-binding ablation does not change biodistribution and toxicity of adenoviral vectors. Gene Ther. **8,** 1347–1353.

ALEMANY, R., SUZUKI, K., and CURIEL, D.T. (2000). Blood clearance rates of adenovirus type 5 in mice. J. Gen. Virol. **81,** 2605–2609.

ASAOKA, K., TADA, M., SAWAMURA, Y., IKEDA, J., and ABE, H. (2000). Dependence of efficient adenoviral gene delivery in malignant glioma cells on the expression levels of the coxsackievirus and adenovirus receptor. J. Neurosurg. **92,** 1002–1008.

BERGELSON, J.M., CUNNINGHAM, J.A., DROGUETT, G., KURT-JONES, E.A., KRITHIVAS, A., HONG, J.S., HORWITZ, M.S., CROWELL, R.L., and FINBERG, R.W. (1997). Isolation of a common receptor for coxsackie B viruses and adenoviruses 2 and 5. Science **275,** 1320–1323.

BEWLEY, M.C., SPRINGER, K., ZHANG, Y.B., FREIMUTH, P., and FLANAGAN, J.M. (1999). Structural analysis of the mechanism of adenovirus binding to its human cellular receptor, CAR. Science **286,** 1579–1583.

DE GEEST, B., SNOEYS, J., VAN LINTHOUT, S., LIEVENS, J., and COLLEN, D. (2005). Elimination of innate immune responses and liver inflammation by PEGylation of adenoviral vectors and methylprednisolone. Hum. Gene Ther. **16,** 1439–1451.

EINFELD, D.A., SCHROEDER, R., ROELVINK, P.W., LIZONOVA, A., KING, C.R., KOVESDI, I., and WICKHAM, T.J. (2001). Reducing the native tropism of adenovirus vectors requires removal of both CAR and integrin interactions. J. Virol. **75,** 11284–11291.

FECHNER, H., HAACK, A., WANG, H., WANG, X., EIZEMA, K., PAUSCHINGER, M., SCHOEMAKER, R., VEGHEL, R., HOUTSMULLER, A., SCHULTHEISS, H.P., LAMERS, J., and POLLER, W. (1999). Expression of coxsackie adenovirus receptor and α_V-integrin does not correlate with adenovector targeting *in vivo* indicating anatomical vector barriers. Gene Ther. **6,** 1520–1535.

HEFFELFINGER, S.C., HAWKINS, H.H., BARRISH, J., TAYLOR, L., and DARLINGTON, G.J. (1992). SK HEP-1: A human cell line of endothelial origin. In Vitro Cell Dev. Biol. **28A,** 136–142.

HONG, S., MAGNUSSON, M., HENNING, P., LINDHOLM, L., and BOULANGER, P. (2003). Adenovirus stripping: A versatile method to generate adenovirus vectors with new cell target specificity. Mol. Ther. **1,** 692–699.

KIRBY, I., DAVISON, E., BEAVIL, A., SOH, C., WICKHAM, T., ROELVINK, P., KOVESDI, I., SUTTON, B., and SANTIS, G. (1999). Mutations in the DG loop of adenovirus type 5 fiber knob protein abolish high-affinity binding to its cellular receptor CAR. J. Virol. **11,** 9508–9514.

KOIVUNEN, E., WANG, B., and RUOSLAHTI, E. (1995). Phage libraries displaying cyclic peptides with different ring sizes: Ligand specificities of the RGD-directed integrins. Biotechnology **13,** 265–270.

KOIZUMI, N., MIZUGUCHI, H., HOSONO, T., ISHII-WATABE, A., UCHIDA, E., UTOGUCHI, N., WATANABE, Y., and HAYAKAWA, T. (2001). Efficient gene transfer by fiber-mutant adenoviral vectors containing RGD peptide. Biochim. Biophys. Acta **1568,** 13–20.

KOIZUMI, N., MIZUGUCHI, H., SAKURAI, F., YAMAGUCHI, T., WATANABE, Y., and HAYAKAWA, T. (2003a). Reduction of natural adenovirus tropism to mouse liver by fiber-shaft exchange in combination with both CAR- and α_V integrin-binding ablation. J. Virol. **77,** 13062–13072.

KOIZUMI, N., MIZUGUCHI, H., UTOGUCHI, N., WATANABE, Y., and HAYAKAWA, T. (2003b). Generation of fiber-modified adenovirus vectors containing heterologous peptides in both the HI loop and C terminus of the fiber knob. J. Gene Med. **5,** 267–276.

KRASNYKH, V., DOUGLAS, J., and VAN BEUSECHEM, W. (2000). Genetic targeting of adenoviral vectors. Mol. Ther. **1,** 391–405.

LEISSNER, P., LEGRAND, V., SCHLESINGER, Y., HADJI, D.A., VAN RAAIJ, M., CUSACK, S., PAVIRANI, A., and MEHTALI, M. (2001). Influence of adenoviral fiber mutations on viral encapsidation, infectivity and *in vivo* tropism. Gene Ther. **8,** 49–57.

LIEBER, A., HE, C., MEUSE, L., SCHOWALTER, D., KIRILLOVA, I., WINTHER, B., and KAY, M. (1997). The role of Kupffer cell activation and viral gene expression in early liver toxicity after infusion of recombinant adenovirus vectors. J. Virol. **71,** 8798–8807.

LIEVENS, J., SNOEYS, J., VEKEMANS, K., VAN LINTHOUT, S., DE ZANGER, R., COLLEN, D., WISSE, E., and DE GEEST, B. (2004). The size of sinusoidal fenestrae is a critical determinant of hepatocyte transduction after adenoviral gene transfer. Gene Ther. **11,** 1523–1531.

LIU, Q., ZAISS, A., COLARUSSO, P., PATEL, K., HALJAN, G., WICKHAM, T., and MURUVE, D. (2003). The role of capsid–endothelial interactions in the innate immune response to adenovirus vectors. Hum. Gene Ther. **14,** 627–643.

MAIZEL, J.V.J., WHITE, D.O., and SCHARFF, M.D. (1968). The polypeptides of adenovirus. I. Evidence for multiple protein components in the virion and a comparison of types 2, 7A, and 12. Virology **36,** 115–125.

MIYAZAWA, N., CRYSTAL, R., and LEOPOLD, P. (1999). Adenovirus serotype 7 retention in a late endosomal compartment prior to cytosol escape is modulated by fiber protein. J. Virol. **75,** 1387–1400.

MIYAZAWA, N., LEOPOLD, P., HACKETT, N., FERRIS, B., WORGALL, S., FALCK-PEDERSEN, E., and CRYSTAL, R. (2001). Fiber swap between adenovirus subgroups B and C alters intracellular trafficking of adenovirus gene transfer vectors. J. Virol. **73,** 6056–6065.

MIZUGUCHI, H., and HAYAKAWA, T. (2002). Adenovirus vectors containing chimeric type 5 and type 35 fiber proteins exhibit altered and expanded tropism and increase the size limit of foreign genes. Gene **285,** 69–77.

MIZUGUCHI, H., and HAYAKAWA, T. (2004). Targeted adenovirus vectors. Hum. Gene Ther. **15,** 1034–1044.

MIZUGUCHI, H., and KAY, M.A. (1998). Efficient construction of a recombinant adenovirus vector by an improved *in vitro* ligation method. Hum. Gene Ther. **9,** 2577–2583.

MIZUGUCHI, H., and KAY, M.A. (1999). A simple method for constructing E1 and E1/E4 deleted recombinant adenovirus vector. Hum. Gene Ther. **10,** 2013-2017.

MIZUGUCHI, H., KOIZUMI, N., HOSONO, T., UTOGUCHI, N., WATANABE, Y., KAY, M.A., and HAYAKAWA, T. (2001). A simplified system for constructing recombinant adenoviral vectors containing heterologous peptides in the HI loop of their fiber knob. Gene Ther. **8,** 730–735.

MIZUGUCHI, H., KOIZUMI, N., HOSONO, T., ISHII-WATABE, A., UCHIDA, E., UTOGUCHI, N., WATANABE, Y., and HAYAKAWA, T. (2002). CAR- or α_V integrin-binding ablated adenovirus vectors, but not fiber-modified vectors containing RGD peptide, do not change the systemic gene transfer properties in mice. Gene Ther. **9,** 769–776.

MORRAL, N., O'NEAL, W., RICE, K., LELAND, M., PIEDRA, P., AGUILAR-CORDOVA, E., CAREY, K., BEAUDET, A., and LANGSTON, C. (2002). Lethal toxicity, severe endothelial injury, and a threshold effect with high doses of an adenoviral vector in baboons. Hum. Gene Ther. **13,** 143–154.

MURUVE, D. (2004). The innate immune response to adenovirus vectors. Hum. Gene Ther. **15,** 1157–1166.

NAKAMURA, T., SATO, K., and HAMADA, H. (2003). Reduction of natural adenovirus tropism to the liver by both ablation of

fiber–coxsackievirus and adenovirus receptor interaction and use of replaceable short fiber. J. Virol. **77,** 2512–2521.

NICKLIN, S., WU, E., NEMEROW, G., and BAKER, A. (2005). The influence of adenovirus fiber structure and function on vector development for gene therapy. Mol. Ther. **12,** 384–393.

NISHIKAWA, M., TAKEMURA, S., TAKAKURA, Y., and HASHIDA, M. (1998). Targeted delivery of plasmid DNA to hepatocytes *in vivo*: Optimization of the pharmacokinetics of plasmid DNA/galactosylated poly(L-lysine) complexes by controlling their physicochemical properties. J. Pharmacol. Exp. Ther. **287,** 408–415.

PASQUALINI, R., KOIVUNEN, E., and RUOSLAHTI, E. (1997). α_v integrins as receptors for tumor targeting by circulating ligands. Nat. Biotechnol. **15,** 542–546.

PHILPOTT, N., NOCIARI, M., ELKON, K., and FALCK-PEDERSEN, E. (2004). Adenovirus-induced maturation of dendritic cells through a PI3 kinase-mediated TNF-α induction pathway. Proc. Natl. Acad. Sci. U.S.A. **101,** 6200–6205.

REID, T., GALANIS, E., ABBRUZZESE, J., SZE, D., WEIN, L., ANDREWS, J., RANDLEV, B., HEISE, C., UPRICHARD, M., HATFIELD, M., ROME, L., RUBIN, J., and KIRN, D. (2002). Hepatic arterial infusion of a replication-selective oncolytic adenovirus (dl1520): Phase II viral, immunologic, and clinical endpoints. Cancer Res. **62,** 6070–6079.

SAKURAI, F., MIZUGUCHI, H., YAMAGUCHI, T., and HAYAKAWA, T. (2003). Characterization of *in vitro* and *in vivo* gene transfer properties of adenovirus serotype 35 vector. Mol. Ther. **8,** 813–821.

SCHIEDNER, G., BLOCH, W., HERTEL, S., JOHNSTON, M., MOLOJAVYI, A., DRIES, V., VARGA, G., VAN ROOIJEN, N., and KOCHANEK, S. (2003). A hemodynamic response to intravenous adenovirus vector particles is caused by systemic Kupffer cell-mediated activation of endothelial cells. Hum. Gene Ther. **14,** 1631–1641.

SCHNELL, M., ZHANG, Y., TAZELAAR, J., GAO, G., YU, Q., QIAN, R., CHEN, S., VARNAVSKI, A., LECLAIR, C., RAPER, S., and WILSON, J. (2001). Activation of innate immunity in nonhuman primates following intraportal administration of adenoviral vectors. Mol. Ther. **3,** 708–722.

SHAYAKHMETOV, D., GAGGAR, A., NI, S., LI, Z., and LIEBER, A. (2005). Adenovirus binding to blood factors results in liver cell infection and hepatotoxicity. J. Virol. **72,** 7478–7491.

SMITH, T., IDAMAKANTI, N., KYLEFJORD, H., ROLLENCE, M., KING, L., KALOSS, M., KALEKO, M., and STEVENSON, S.C. (2002). *In vivo* hepatic adenoviral gene delivery occurs independently of the coxsackievirus–adenovirus receptor. Mol. Ther. **5,** 770–779.

SMITH, T., IDAMAKANTI, N., ROLLENCE, M.L., MARSHALL-NEFF, J., KIM, J., MULGREW, K., NEMEROW, G.R., KALEKO, M., and STEVENSON, S.C. (2003a). Adenovirus serotype 5 fiber shaft influences *in vivo* gene transfer in mice. Hum. Gene Ther. **14,** 777–787.

SMITH, T., IDAMAKANTI, N., MARSHALL-NEFF, J., ROLLENCE, M., WRIGHT, P., KALOSS, M., KING, L., MECH, C., DINGES, L., IVERSON, W., SHERER, A., MARKOVITS, J., LYONS, R., KALEKO, M., and STEVENSON, S. (2003b). Receptor interactions involved in adenoviral-mediated gene delivery after systemic administration in non-human primates. Hum. Gene Ther. **14,** 1595–1604.

TOMKO, R.P., XU, R., and PHILIPSON, L. (1997). HCAR and MCAR: The human and mouse cellular receptors for subgroup C adenoviruses and group B coxsackieviruses. Proc. Natl. Acad. Sci. U.S.A. **94,** 3352–3356.

VIGNE, E., DEDIEU, J., BRIE, A., GILLARDEAUX, A., BRIOT, D., BENIHOUD, K., LATTA-MAHIEU, M., SAULNIER, P., PERRICAUDET, M., and YEH, P. (2003). Genetic manipulations of adenovirus type 5 fiber resulting in liver tropism attenuation. Gene Ther. **10,** 153–162.

WICKHAM, T.J. (2000). Targeting adenovirus. Gene Ther. **7,** 110–114.

WICKHAM, T.J., MATHIAS, P., CHERESH, D.A., and NEMEROW, G.R. (1993). Integrins $\alpha_v\beta_3$ and $\alpha_v\beta_5$ promote adenovirus internalization but not virus attachment. Cell **73,** 309–319.

WICKHAM, T.J., FILARDO, E.J., CHERESH, D.A., and NEMEROW, G.R. (1994). Integrin $\alpha_v\beta_5$ selectively promotes adenovirus mediated cell membrane permeabilization. J. Cell Biol. **127,** 257–264.

XU, Z.-L., MIZUGUCHI, H., ISHII-WATABE, A., UCHIDA, E., MAYUMI, T., and HAYAKAWA, T. (2001). Optimization of transcriptional regulatory elements for constructing plasmid vectors. Gene **272,** 149–156.

ZINN, K., SZALAI, A., STARGEL, A., KRASNYKH, V., and CHAUDHURI, T. (2004). Bioluminescence imaging reveals a significant role for complement in liver transduction following intravenous delivery of adenovirus. Gene Ther. **11,** 1482–1486.

ZSENGELLER, Z., OTAKE, K., HOSSAIN, S.A., BERCLAZ, P.Y., and TRAPNELL, B.C. (2000). Internalization of adenovirus by alveolar macrophages initiates early proinflammatory signaling during acute respiratory tract infection. J. Virol. **74,** 9655–9667.

Address reprint requests to:
Dr. Hiroyuki Mizuguchi
National Institute of Biomedical Innovation
Asagi 7-6-8, Saito
Ibaraki, Osaka 567-0085, Japan

E-mail: mizuguch@nibio.go.jp

Received for publication August 3, 2005; accepted after revision December 9, 2005.

Published online: February 8, 2006.

0022-3565/06/3161-255–260$20.00
THE JOURNAL OF PHARMACOLOGY AND EXPERIMENTAL THERAPEUTICS

JPET 316:255–260, 2006

Vol. 316, No. 1
93351/3066944
Printed in U.S.A.

Preparation of a Claudin-Targeting Molecule Using a C-Terminal Fragment of *Clostridium perfringens* Enterotoxin

Chiaki Ebihara, Masuo Kondoh, Naoki Hasuike, Motoki Harada, Hiroyuki Mizuguchi, Yasuhiko Horiguchi, Makiko Fujii, and Yoshiteru Watanabe

Department of Pharmaceutics and Biopharmaceutics, Showa Pharmaceutical University, Machida, Tokyo, Japan (C.E., M.K., N.H., M.H., M.F., Y.W.); Graduate School of Pharmaceutical Sciences, Osaka University, Suita, Osaka, Japan (H.M.); Laboratory of Gene Transfer and Regulation, National Institute of Biomedical Innovation, Ibaraki, Osaka, Japan (H.M.); and Department of Bacterial and Toxinology, Division of Infectious Diseases, Osaka University, Suita, Osaka, Japan (Y.H.)

Received July 26, 2005; accepted September 2, 2005

ABSTRACT

Although most malignant tumors are epithelia-derived carcinomas, methods for specific and effective delivery of antitumor agents to carcinomas have not been developed. Recent reports indicate that epithelia overexpress claudin-3 and -4, which are integral membrane proteins of epithelial tight junctions. This suggests that claudins can be targeted for tumor therapy, but there is not currently a method for delivering drugs to claudin-expressing cells. In the present study, we evaluated whether a potent claudin-4-binding C-terminal fragment of *Clostridium perfringens* enterotoxin (C-CPE) would allow targeting to claudin-4-expressing cells. We fused C-CPE to the protein synthesis inhibitory factor (PSIF), which lacks the cell binding domain of *Pseudomonas* exotoxin. This fusion protein, C-CPE-PSIF, was cytotoxic to MCF-7 human breast cancer cells, which express endogenous claudin-4, but it was not toxic to mouse fibroblast L cells, which lack endogenous claudin-4. The cytotoxicity of C-CPE-PSIF was attenuated by pretreating the MCF-7 cells with C-CPE but not bovine serum albumin. Also, deletion of the claudin-4-binding region of C-CPE reduced the cytotoxicity of C-CPE-PSIF. Finally, we found that C-CPE-PSIF is toxic to L cells expressing claudin-4 but not to normal L cells or cells expressing claudin-1, -2, or -5. These results indicate that use of the C-CPE peptide may provide a novel way to target drugs to claudin-expressing cells.

Epithelial-derived tumors account for 90% of all malignant tumors, and their resistance to chemotherapy is a major clinical problem (Greenlee et al., 2000). Recent progress in combinatorial chemistry, proteomics, and genomics research has further advanced the development of effective drugs against carcinomas, but, for clinical application, it is also essential to develop selective and efficient drug delivery systems for these novel drugs (Allen and Cullis, 2004).

These drugs can be delivered by targeting several cell surface molecules, including carcinoembryonal antigen, carboanhydrage IX, and epithelial cell adhesion molecule (Steffens et al., 1997; Chester et al., 2000; Mayer et al., 2000; McLaughlin et al., 2001). In fact, experimental therapies have been developed using antibody-mediated targeting of these molecules. However, because carcinoembryonal antigen and carboanhydrage IX are expressed by carcinomas as well as normal epithelium in kidney and liver, side effects are difficult to avoid (Steffens et al., 1997; Chester et al., 2000; Mayer et al., 2000). Moreover, the antibody for epithelial cell adhesion molecule itself is toxic to normal epithelium (McLaughlin et al., 2001).

Tight junctions (TJs), which are points of intercellular contact and interaction, are characteristic and complex structures in the epithelia. TJs play a critical role in forming a barrier between apical and basal sides of the cell, and they are present on the lateral side of the cell where they mediate intercellular interactions (Schneeberger and Lynch, 2004). Loss of polarity is a typical feature of transformation in epithelial cells. Furthermore, abnormal localization of membrane proteins, including TJ components, adherence junction proteins, and apical and basal proteins, is observed during carcinogenesis (Wodarz, 2000; Yarden and Sliwkowski, 2001; Vermeer et al., 2003). These findings indicate that abnor-

This work was partly supported by a grand-in-aid of the Ministry of Education, Sports and Science in Japan.
C.E. and M.K. contributed equally to this work.
Article, publication date, and citation information can be found at http://jpet.aspetjournals.org.
doi:10.1124/jpet.105.093351.

ABBREVIATIONS: TJ, tight junction; CPE, *C. perfringens* enterotoxin; C-CPE, C-terminal fragment of *C. perfringens* enterotoxin; PSIF, protein synthesis inhibitory factor derived from *Pseudomonas* exotoxin; PE, *Pseudomonas* exotoxin; C-CPE-PSIF, C-terminal fragment of *C. perfringens* enterotoxin fused to a protein synthesis inhibitory factor; BSA, bovine serum albumin; PCR, polymerase chain reaction; PBS, phosphate-buffered saline; PAGE, polyacrylamide gel electrophoresis; LDH, L-lactate dehydrogenase.

mally localized membrane proteins may be useful for targeting drugs to carcinoma cells.

Claudin is an approximately 23-kDa transmembrane protein found in the TJ, and it plays a pivotal role in the barrier function of the TJ (Tsukita et al., 2001). There are more than 20 members of claudin family, and they are expressed in a tissue-specific manner (Morita et al., 1999a,b). For instance, claudin-1 is ubiquitously expressed, and claudin-3 is observed in the lung and liver. In mice, claudin-5 is expressed in all blood endothelial cells. Claudin-6 is widely expressed only in the fetus. Interestingly, the overexpression of claudins is frequently observed in the epithelium of ovarian cancer, hepatocellular carcinoma, malignant pancreatic cancer, and prostate cancer (Hough et al., 2000; Long et al., 2001; Michl et al., 2003; Rangel et al., 2003; Cheung et al., 2005). Therefore, claudins are promising candidates for the targeting of anticancer drugs to carcinoma cells.

Clostridium perfringens enterotoxin (CPE) is a single polypeptide with a molecular mass of 35 kDa that causes food poisoning associated with most human food-borne illnesses (McClane and Chakrabarti, 2004). CPE is made up of two functionally distinct domains: an approximately 22-kDa N-terminal domain that mediates cytotoxicity and an approximately 13-kDa C-terminal domain (C-CPE) that mediates binding (McClane and Chakrabarti, 2004). Claudin-3 and -4 are the receptors for CPE (Katahira et al., 1997; Sonoda et al., 1999), and we and others have shown that they bind to CPE via the C-CPE domain (Katahira et al., 1997; Sonoda et al., 1999; Fujita et al., 2000; Kondoh et al., 2005). These findings suggest that CPE could be used for the targeting of claudins on epithelial carcinoma cells. Indeed, CPE has been successfully used to treat human ovarian and pancreatic cancers, both of which express high levels of claudin-3 or -4 (Michl et al., 2001; Santin et al., 2005).

In the present study, we investigated whether C-CPE can be used to target claudin-4-expressing cells. For this purpose, we utilized a PSIF derived from PE as a reporter molecule (Leamon et al., 1993; Mesri et al., 1994; Beers et al., 2000) to assess targeting of claudin-4-expressing cells. PE (GenBank accession no. K01397; http://www.ncbi.nlm.nih.gov/entrez/viewer.fcgi?db=nucleotide&val=151215) binds to the cell surface and is internalized via the endocytotic pathway, after which it escapes from endosomes into the cytosol. The PE fragments (PSIF) released into the cytosol inhibit protein synthesis by blocking the function of elongation factor 2 (Ogata et al., 1990). The PSIF, which cannot invade into cells, does not show any cytotoxicity because of lacking the cell binding domain. We show here that a C-CPE-PSIF fusion was toxic to cells expressing claudin-4 but not to cells expressing claudin-1. In addition, the cytotoxic effects of C-CPE-PSIF were dose dependently attenuated by C-CPE. Thus, C-CPE is a potent molecule for targeting of claudin-4-expressing cells and should be useful as a system for delivering drugs against malignant carcinomas.

Materials and Methods

Chemicals. Anti-FLAG M2 affinity gel, anti-FLAG M2 monoclonal antibody-peroxidase conjugate, FLAG peptide, and bovine serum albumin (BSA) were purchased from Sigma-Aldrich (St. Louis, MO). Glutathione-Sepharose 4B resin, thrombin protease, and Benzamidine-Sepharose 4 Fast Flow were obtained from GE Healthcare (Little Chalfont, Buckinghamshire, UK). Horseradish peroxidase-labeled Ab, anti-claudin-1 pAb, anti-claudin-2 pAb, anti-claudin-4 mAb, anti-claudin-5 mAb, and anti β-actin mAb were obtained from Zymed Laboratories (South San Francisco, CA). All other reagents used were research grade.

Cell Culture. Human breast cancer cell line MCF-7 cells and human intestinal cell line Caco-2 cells were maintained in RPMI 1640 medium and Dulbecco's modified Eagle's medium containing 10% fetal calf serum at 37°C, respectively. Mouse fibroblast cell line L cells and mouse claudin-expressing L cells, kindly provided by Dr. S. Tsukita (Kyoto University, Japan) (Morita et al., 1999b; Sonoda et al., 1999), were cultured in modified Eagle's medium containing 10% fetal calf serum at 37°C.

Preparation of C-CPE-PSIF Fusions. The plasmids containing fusions of PSIF with C-CPE and C-CPE lacking its C-terminal 30 amino acids (C-CPE289) were prepared as follows. C-CPE and C-CPE289 were amplified by polymerase chain reaction (PCR) using pET16bHis$_{10}$C-CPE as a template (Katahira et al., 1997), a common forward primer (5′-CCATGGCCGAGAGATGTGTTTTAACAGTT-3′, NcoI site is underlined), and a reverse primer for C-CPE (5′-GCGGCCGCAAATTTTTGAAATAATATTGA-3′, NotI site is underlined) or C-CPE289 (5′-GCGGCCGCTATATCAACATAATGATCTTT-3′, NotI site is underlined). The resulting PCR fragments were subcloned into the pGEM T-Easy Vector to create pTA/C-CPE and pTA/C-CPE289 (Promega, Madison, WI), and the sequences were confirmed. PSIF was amplified using PSIF primer-1 (5′-GATGATCGATCGCGGCCGCAGGTGCGCCGGTGCCGTATCCGGATCCGCTGGAACCGCGTGCCGCA*GACTACAAAGACGACGACGACAAA*CCCGAGGGCGGCAGCCTGGCCGCGCTGACC-3′, the underline indicates the NotI site, and the italic letters indicate the FLAG sequence), PSIF primer-2 (5′-GATCGATCGATCACTAGTCTACAGTTCGTCTTTCTTCAGGTCCTCGCGCGGCGGTTTGCCGGG-3′, the underline indicates SpeI site), and *Pseudomonas aerginosa* cDNA as a template. The resulting PCR products were subcloned into the pGEM T-Easy Vector, and the sequences were confirmed. The NotI/SpeI-digested PSIF fragment was inserted into the NotI/SpeI-digested pY02 (Yamamoto et al., 2003) to generate pY02-PSIF. The pTA/C-CPE and pTA/C-CPE289 plasmids were digested with NotI and NcoI, and the fragments were inserted into NotI/NcoI-digested pY02-PSIF to generate pY02-C-CPE-PSIF and pY02-C-CPE289-PSIF. The C-CPE-PSIF plasmids were transduced into *Escherichia coli* strain TG1, after which the cells were grown at 37°C in 2YT medium (Invitrogen, Carlsbad, CA) containing 2% glucose to an optical density at 600 nm of 0.6 to 0.9. The medium was then changed to 2YT medium containing 1 mM isopropyl β-D-thiogalactopyranoside. After an additional 18 h of culture at 30°C, the cells were harvested and centrifuged. The resulting supernatant was applied to anti-FLAG M2 affinity gel, and the bound proteins were eluted with FLAG peptide. The buffer was exchanged with phosphate-buffered saline (PBS) using a PD-10 column (GE Healthcare), and the purified protein was stored at −80°C until use. Purification of the of C-CPE-PSIF proteins was confirmed by SDS-polyacrylamide gel electrophoresis (PAGE), followed by staining with Coomassie Brilliant Blue and by immunoblotting with anti-FLAG M2 antibody (Fig. 1; data not shown). Protein was quantified using a commercially available assay kit with BSA as a standard (Bio-Rad, Hercules, CA).

Preparation of C-CPE. Following digestion of pTA/C-CPE with XhoI and NotI, the resulting DNA fragments were inserted into XhoI/NotI-digested pGEX4T-1 (GE Healthcare). Glutathione *S*-transferase-fused C-CPE was prepared as follows. The pGEX4T-1 plasmid encoding C-CPE was transduced into *E. coli* BL21 (DE3), after which the cells were cultured in LB medium at 37°C until the logarithmic phase. The culture was then adjusted to 1 mM isopropyl β-D-thiogalactopyranoside, and the cells were grown for an additional 6 h. The cells were harvested and then solubilized in lysis buffer (10 mM Tris-HCl, 150 mM NaCl, and 1 mM EDTA, pH 8.0) containing 100 μg/ml lysozyme, 5 mM dithiothreitol, and 1.5% *N*-lauroylsarcosine. The lysate was centrifuged, after which the super-

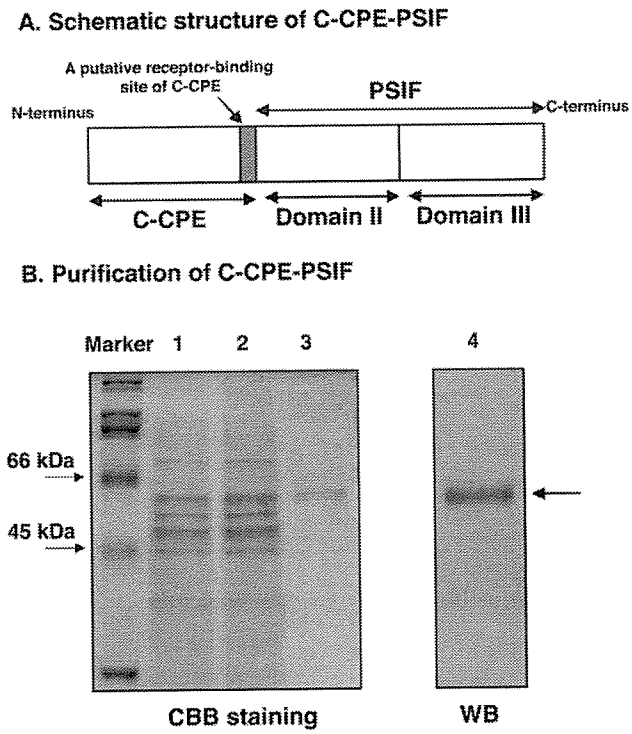

Fig. 1. Preparation of C-CPE-PSIF. A, schematic structure of C-CPE-PSIF. C-CPE-PSIF is a fusion of C-CPE and PSIF. The putative receptor-binding region of C-CPE is located in its C terminus and is shown here as the dark area (Hanna et al., 1991). PSIF contains domains II and III of PE. Domain II is critical for escape of the toxin from the endosome to the cytosol, and domain III is responsible for inhibition of protein synthesis (Ogata et al., 1990). B, purification of C-CPE-PSIF. C-CPE-PSIF was expressed in *E. coli* and isolated by anti-FLAG affinity chromatography. The purification of C-CPE-PSIF was confirmed by SDS-PAGE followed by staining with Coomassie Brilliant Blue (CBB) (lanes 1–3) and by immunoblotting using an antibody against FLAG (lane 4). The arrow indicates the purified C-CPE-PSIF. Lane 1, *E. coli* lysates; lane 2, flow-through; lanes 3 and 4, eluted fraction.

natant was collected and adjusted to 2% Triton X-100. The supernatant was incubated with glutathione-agarose beads for 2 h at 4°C. The beads were then washed with the lysis buffer, and C-CPE was eluted from the beads by cleavage with thrombin. Thrombin was removed from the eluted protein using Benzamidine-Sepharose 4 Fast Flow. The buffer was then exchanged with PBS using a PD-10 column. The purification of C-CPE was confirmed by SDS-PAGE (data not shown).

Trypan Blue Assay. Cells were treated with vehicle or C-CPE-PSIF proteins for the indicated periods. Both the floating and adherent cells were recovered and were suspended in ice-cold PBS. The cell suspension was adjusted to 0.2% trypan blue, and the number of stained (dying or dead) and unstained (living) cells was counted. At least 300 cells were counted to determine the fraction of dead cells.

L-Lactate Dehydrogenase Release Assay. The release of lactate dehydrogenase (LDH) from the cells was analyzed using a CytoTox96 NonRadioactive Cytotoxicity Assay kit (Promega) according to the manufacturer's protocol. LDH release was calculated using the following equation: percentage of maximal LDH release = LDH in the cultured medium/total LDH in the culture dish.

Competition Assay. MCF-7 cells were pretreated with C-CPE or BSA at the indicated concentration for 1 h, after which C-CPE-PSIF was added to the cells. After an additional 36 h of culture, LDH release was assayed as described above.

Statistical Analysis. Statistical significance of differences was assessed using one-way analysis of variance followed by Dunnett's test. Differences were considered significant when $p < 0.05$.

Results

Preparation of C-CPE-PSIF. To assess the ability of C-CPE to target claudin-4-expressing cells, we fused it with PSIF. Because of limitations of the restriction sites in the PSIF-encoding plasmid, we linked C-CPE to a site upstream of the 5′ terminus of PSIF (Fig. 1A). As shown in Fig. 1B, C-CPE-PSIF was produced effectively by *E. coli* and could be purified by affinity chromatography using anti-FLAG antibodies. Its molecular size as determined by SDS-PAGE was identical to its predicted size (58 kDa).

Cytotoxic Properties of C-CPE-PSIF. To examine the cytotoxic properties and specificity of C-CPE-PSIF, we compared its effects on L cells, which lack endogenous claudins, and MCF-7 cells, which express endogenous claudin-4 (Fig. 2A). Trypan blue dye exclusion showed C-CPE-PSIF caused

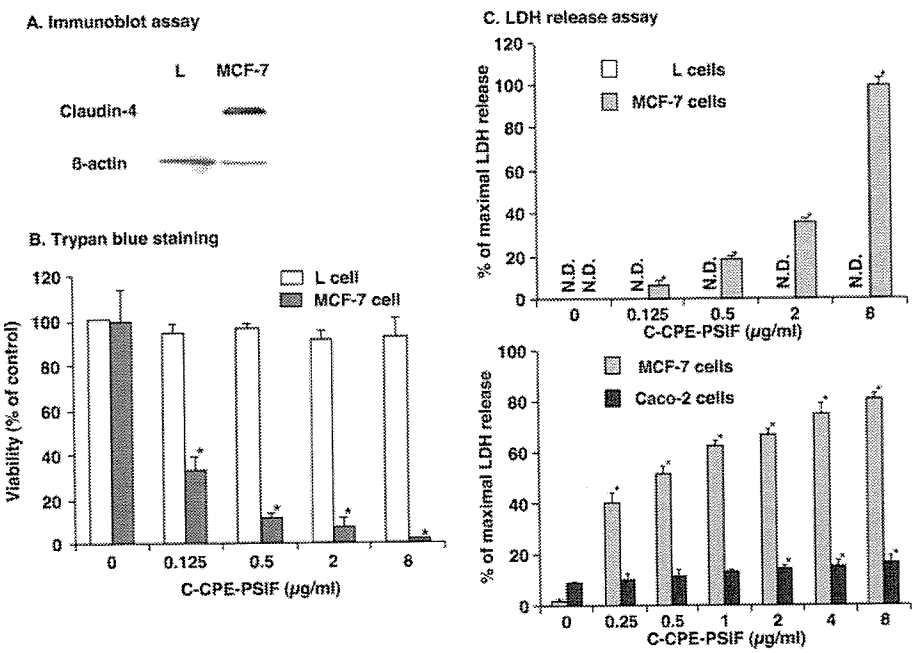

Fig. 2. Cytotoxicity of C-CPE-PSIF. A, expression of claudin-4 in L and MCF-7 cells. Claudin-4 expression was assessed by immunoblotting. Blots were also probed with a β-actin antibody to show equivalent loading. B, trypan blue assay. The cells were treated with C-CPE-PSIF at the indicated concentrations for 36 h. The cells were then harvested and stained with 0.2% trypan blue. The blue-stained cells (dead and dying cells) and the unstained cells (living cells) were counted under a microscope. At least 300 cells were counted in each condition. Results indicate the means ± S.D. ($n = 3$). *, significantly different from the vehicle-treated cells ($P < 0.05$). C, LDH release assay. Cells were treated for 36 h with the indicated concentrations of C-CPE-PSIF, after which the rate of LDH release was determined. There was no LDH release from the C-CPE-PSIF-treated L cells. Results represent means ± S.D. ($n = 3$). *, significantly different from the vehicle-treated cells ($P < 0.05$). N.D., not detected.

dose-dependent cell death in MCF-7 cells, with 92% death after a 36-h treatment with 2 μg/ml C-CPE-PSIF (Fig. 2B). Similar results were observed in the LDH release assay. In this case, 8 μg/ml C-CPE-PSIF caused the release of approximately 100% of the LDH (Fig. 2C). In contrast, even at 8 μg/ml, C-CPE/PSIF was not cytotoxic to L cells and Caco-2 cells (Fig. 2, B and C). Taken together, these results suggested that C-CPE-PSIF is toxic to claudin-4-expressing tumor epithelial cells.

Targeting Properties of C-CPE-PSIF. We next used a competition assay to determine whether C-CPE-PSIF binds to MCF-7 cells via C-CPE. As shown in Fig. 3A, pretreatment of the cells with C-CPE dose dependently attenuated the cytotoxic activity of 0.5 μg/ml C-CPE-PSIF, with a maximal effect observed at 5 μg/ml C-CPE. In contrast, pretreatment of the cells with 10 μg/ml BSA did not reduce the cytotoxicity of 0.5 μg/ml C-CPE/PSIF. These results suggest that C-CPE-PSIF interacts with MCF-7 cells via the C-CPE domain.

C-CPE is known to bind to claudin-4 via its 30 C-terminal acids (Kondoh et al., 2005). To confirm that claudin-4 is involved in the cytotoxicity of C-CPE-PSIF, we prepared C-CPE289-PSIF, which lacks the claudin-4-binding region of C-CPE. As expected, C-CPE-PSIF had a powerful toxic effect on MCF-7 cells, reaching 70% cell death at 4 μg/ml. In contrast, even at 8 μg/ml, C-CPE289-PSIF was not cytotoxic. These results suggested that interaction with claudin-4 is essential for the cytotoxicity of C-CPE-PSIF.

To confirm this possibility, we evaluated the cytotoxic activity of C-CPE-PSIF in L cells expressing claudin-1 (CL1/L cells), -2 (CL2/L cells), -4 (CL4/L cells), and -5 (CL5/L cells) (Figs. 4, B and C). C-CPE-PSIF was not cytotoxic in CL1/L, CL2/L, and CL5/L cells (Fig. 4C), and it was toxic in CL4/L cells (31.3 and 73.5% LDH release at 0.1 and 5 μg/ml, respectively). These results confirm that the C-CPE domain of C-CPE-PSIF interacts with claudin-4 on the cell membrane.

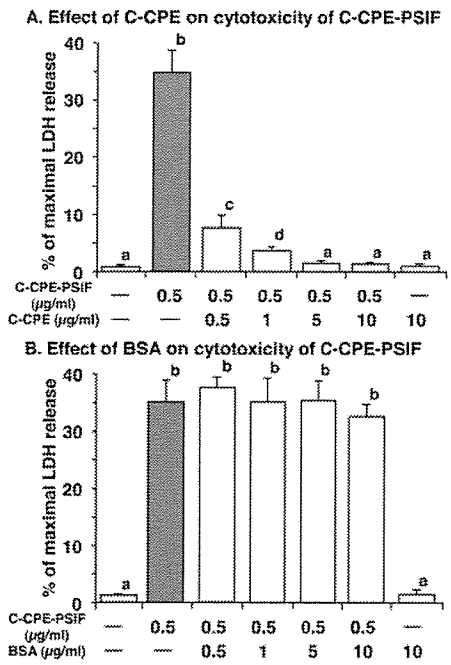

Fig. 3. C-CPE-PSIF interacts with cells via the C-CPE domain. MCF-7 cells were treated with the indicated concentrations of C-CPE (A) or BSA (B) for 1 h. The cells were then treated for 36 h with 0.5 μg/ml C-CPE-PSIF, after which LDH release was assessed. Results represent the means ± S.D. (n = 3). There were significant differences between conditions with the different superscripts ($P < 0.05$).

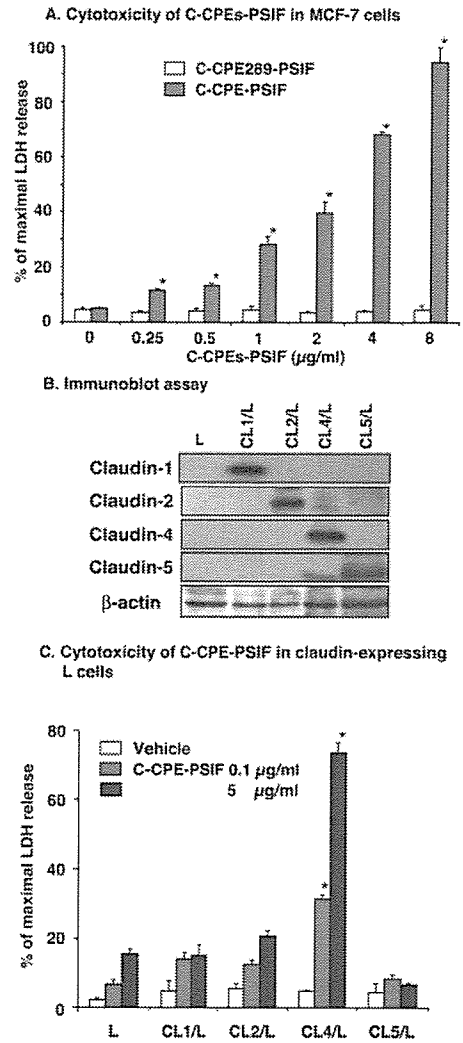

Fig. 4. Involvement of claudin-4 in the cytotoxicity of C-CPE-PSIF. A, cytotoxicity of C-CPE289-PSIF in MCF-7 cells. MCF-7 cells were treated for 36 h with the indicated concentrations of C-CPE289-PSIF or C-CPE-PSIF, after which LDH release was assessed. The results represent the means ± S.D. (n = 3). *, significantly different from the vehicle-treated cells ($P < 0.05$). B, immunoblot analysis of claudin-expressing L cells. The expression profiles for claudin family members were determined by immunoblotting. C, cytotoxicity of C-CPE-PSIF in claudin-expressing L cells. L cells expressing claudins were treated for 36 h with the indicated concentrations of C-CPE-PSIF, after which LDH release was assessed. Results represent the means ± S.D. (n = 3). *, significantly different from the L cells ($P < 0.05$).

Discussion

In the current studies, we found that a C-CPE-PSIF fusion protein is potently cytotoxic to claudin-4-expressing cells. This suggests that C-CPE could be used to confer claudin binding to drugs.

We used a fusion in which the C terminus of C-CPE was linked to the N terminus of PSIF. Thus, the receptor-binding region of C-CPE may be influenced by fusion with PSIF. To investigate this further, we are currently attempting to prepare C-CPE-PSIF with a G4S linker inserted between the C-CPE and PSIF domains. In the current studies, it was necessary to connect PSIF to the C terminus of C-CPE be-

cause of technical aspects of plasmid construction, and we need to consider the function of C-CPE when preparing other claudin-4-targeting molecules. Solution of the three-dimensional structures of claudins and CPE should be helpful. Competitive analysis using C-CPE revealed that C-CPE-PSIF interacted with cells via the C-CPE domain. Thus, cellular uptake of C-CPE-PSIF appears to be dependent on the interaction of claudin-4 with C-CPE. Indeed, we found that L cells expressing claudin-1, -2, or -5 are insensitive to C-CPE-PSIF and that deletion of the claudin-4-binding domain of C-CPE eliminates its cytotoxicity. These results indicate that C-CPE-PSIF binds to claudin-4 on the cell surface. Similarly, Fujita et al. (2000) showed that CPE binds to claudin-4 but not claudin-1, -2, or -5. Also, expression of claudin-4 but not -1 or -5 confers sensitivity to CPE (Sonoda et al., 1999; Fujita et al., 2000). Thus, our data are consistent with previous findings, and they show that fusion with C-CPE, the receptor-binding region of CPE, confers claudin binding to PSIF. The receptor-binding region of CPE was previously narrowed to the C-terminal 30 amino acids (Hanna et al., 1991). Similarly, we reported that deletion of the C-terminal 30 amino acids of C-CPE eliminates its ability to bind claudin-4 (Kondoh et al., 2005). Here, we showed that deletion of the 30 amino acids in C-CPE-PSIF abolishes its toxic effects. Taken together, the results indicate that C-CPE could be used to target drugs to claudin-4.

For the use of claudins as targets for drug delivery, it is important to understand whether molecules binding to claudin on the cell surface are taken up into the cells. PSIF is a useful as a reporter for screening ligands (Siegall et al., 1990; Theuer et al., 1992; Leamon et al., 1993). Because C-CPE-PSIF was cytotoxic in claudin-4-expressing cells, we expect that C-CPE-PSIF must enter the cytosol. This leaves the question of how C-CPE-PSIF enters the cells. One possibility is that it is taken up by endocytosis, after which it escapes from the endosomes into the cytosol. Generally, proteins are targeted to clathrin-coated vesicles by a sorting signal sequence, including YXXØ or EXXXLL (where X is any amino acid, and Ø is a bulky hydrophobic residue) (Bonifacino and Traub, 2003). Because claudin-4 contains an ALGVLL motif at amino acids 92 to 97 and a YVGW motif at amino acids 165 to 168 (Ivanov et al., 2004), it may be taken up by clathrin-mediated endocytosis. Indeed, Matsuda et al. (2004) showed that the endocytosis of claudins occurs during the remodeling of TJs.

Claudins are overexpressed in some tumor cells. Administration of CPE has been shown to reduce the growth of claudin-4-overexpressing human ovarian and pancreatic tumors (Michl et al., 2001; Rangel et al., 2003; Santin et al., 2005). CPE contains not only a claudin-4-binding domain but also a cytotoxic domain (McClane and Chakrabarti, 2004). Therefore, it is hard to use CPE in itself as a targeting molecule to claudin-4. Offner et al. (2005) reported that antibodies for claudins bind to claudin-expressing carcinomas, suggesting that anti-claudin antibodies or their F_v domains could be used to target antitumor agents to claudin-positive tumors. However, targeting of an antitumor agent to cells via a claudin has never been achieved. In this point, C-CPE is a useful claudin-4-targeting molecule, and C-CPE could target not only antitumor agents but also liposomes to claudin-4-overexpressing tumor cells. Although claudin-4 is also distributed in normal tissues such as normal colon epithelium and several glands, the expression in normal tissues is weaker than in tumors (Long et al., 2001; Michl and Gress, 2004). Therefore, detailed analysis for mechanism of interaction between C-CPE and claudin-4 is needed for a future application of antitumor therapy using C-CPE. In the present study, we found that C-CPE-PSIF was nontoxic in Caco-2 cells. We previously reported that addition of C-CPE in basal side not apical side of Caco-2 monolayer resulted in decrease of the barrier function of TJ (Masuyama et al., 2005; Takahashi et al., 2005). McClane and Chakrabarti (2004) also reported that Caco-2 cells are more sensitive to CPE when CPE is applied to their basal side than when CPE is applied to their apical sides. Taken together, insensitivity of Caco-2 cells to C-CPE-PSIF may be due to polarization of Caco-2 cells. This is an interesting founding, and it is an important issue to clarify the relationship between sensitivity of C-CPE-PSIF and polarization of claudin-4 in tumor tissues and normal tissues. C-CPE reduced the barrier function of TJ of epithelia (Kondoh et al., 2005), and utilization of C-CPE may facilitate drug delivery to intratumor tissues.

We previously showed that the C-terminal 16 amino acids of C-CPE are responsible for its interaction of claudin-4 (Kondoh et al., 2005), indicating that modification of the C terminus of C-CPE could allow other claudins to be targeted. For example, it may be useful to target claudin-10 because it is overexpressed in hepatocellular carcinomas (Cheung et al., 2005). Because the plasmid encoding C-CPE-PSIF is a phagemid vector, its binding specificity can be easily manipulated using phage display. We are currently attempting to identify the precise claudin-4 binding region of C-CPE and to use a phage display library to prepare versions of C-CPE that can bind other claudins.

In summary, we showed that the C-CPE domain of C-CPE-PSIF targets claudin-4. This is the first report that C-CPE can allow the targeting of a drug to claudin-4. Because of these results, we are currently developing a claudin-targeting drug delivery system.

Acknowledgments

We thank S. Tsukita and Y. Tsutsumi for providing claudin-expressing L cells and pY02 plasmid, respectively. We also thank N. Koizumi, W. Mikami, and A. Takahashi for excellent technical assistance and helpful discussion.

References

Allen TM and Cullis PR (2004) Drug delivery systems: entering the mainstream. *Science (Wash DC)* **303:**1818–1822.

Beers R, Chowdhury P, Binger D, and Pastan I (2000) Immunotoxins with increased activity against epidermal growth factor receptor vIII-expressing cells produced by antibody phage display. *Clin Cancer Res* **6:**2835–2843.

Bonifacino JS and Traub LM (2003) Signals for sorting of transmembrane proteins to endosomes and lysosomes. *Annu Rev Biochem* **72:**395–447.

Chester KA, Mayer A, Bhatia J, Robson L, Spencer DI, Cooke SP, Flynn AA, Sharma SK, Boxer G, Pedley RB, et al. (2000) Recombinant anti-carcinoembryonic antigen antibodies for targeting cancer. *Cancer Chemother Pharmacol* **46 (Suppl):**S8–S12.

Cheung ST, Leung KL, Ip YC, Chen X, Fong DY, Ng IO, Fan ST, and So S (2005) Claudin-10 expression level is associated with recurrence of primary hepatocellular carcinoma. *Clin Cancer Res* **11:**551–556.

Fujita K, Katahira J, Horiguchi Y, Sonoda N, Furuse M, and Tsukita S (2000) *Clostridium perfringens* enterotoxin binds to the second extracellular loop of claudin-3, a tight junction integral membrane protein. *FEBS Lett* **476:**258–261.

Greenlee RT, Murray T, Bolden S, and Wingo PA (2000) Cancer Statistics, *2000 CA Cancer J Clin* **50:**7–33.

Hanna PC, Mietzner TA, Schoolnik GK, and McClane BA (1991) Localization of the receptor-binding region of *Clostridium perfringens* enterotoxin utilizing cloned toxin fragments and synthetic peptides. *J Biol Chem* **266:**11037–11043.

Hough CD, Sherman-Baust CA, Pizer ES, Montz FJ, Im DD, Rosenshein NB, Cho KR, Riggins GJ, and Morin PJ (2000) Large-scale serial analysis of gene expres-